



Contents lists available at ScienceDirect

Animal Nutrition

journal homepage: <http://www.keaipublishing.com/en/journals/aninu/>

Original Research Article

Chronic exposure to high-density polyethylene microplastic through feeding alters the nutrient metabolism of juvenile yellow perch (*Perca flavescens*)



Xing Lu ^{a,1}, Dong-Fang Deng ^{a,*}, Fei Huang ^a, Fabio Casu ^b, Emma Kraco ^a, Ryan J. Newton ^a, Merry Zohn ^c, Swee J. Teh ^d, Aaron M. Watson ^b, Brian Shepherd ^c, Ying Ma ^{a,2}, Mahmoud A.O. Dawood ^{a,3}, Lorena M. Rios Mendoza ^e

^a School of Freshwater Sciences, University of Wisconsin, Milwaukee, WI, 53204, USA

^b South Carolina Department of Natural Resources, Charleston, SC, 29412, USA

^c USDA/ARS/School of Freshwater Sciences, University of Wisconsin, Milwaukee, WI, 53204, USA

^d School of Veterinary Medicine, Department of Anatomy, Physiology, and Cell Biology, University of California, Davis, CA, 95616, USA

^e Department of Natural Sciences, Marine Resources Research Institute, University of Wisconsin, Superior, WI, 54880, USA

ARTICLE INFO

Article history:

Received 2 August 2021

Received in revised form

30 December 2021

Accepted 30 January 2022

Available online 5 February 2022

Keywords:

Dietary exposure

Intestinal microbiota

Liver metabolomics

Microplastics

Nutrient composition

Yellow perch

ABSTRACT

Microplastics are emergent contaminants threatening aquatic organisms including aquacultured fish. This study investigated the effects of high-density polyethylene (HDPE, 100 to 125 μm) on yellow perch (*Perca flavescens*) based on integrative evaluation including growth performance, nutritional status, nutrient metabolism, fish health, and gut microbial community. Five test diets (0, 1, 2, 4, or 8 g HDPE/100 g diet) containing 41% protein and 10.5% lipid were fed to juvenile perch (average body weight, 25.9 ± 0.2 g; $n = 15$) at a feeding rate of 1.5% to 2.0% body weight daily. The feeding trial was conducted in a flow-through water system for 9 wk with 3 tanks per treatment and 15 yellow perch per tank. No mortality or HDPE accumulation in the fish was found in any treatments. Weight gain and condition factor of fish were not significantly impacted by HDPE ($P > 0.05$). Compared to the control group, fish fed the 8% HDPE diet had significantly decreased levels of protein and ash ($P < 0.05$). In response to the increasing levels of HDPE exposure, the hepatosomatic index value, hepatocyte size, and liver glycogen level were increased, but lipid content was reduced in the liver tissues. Compared to the control treatment, fish fed the 8% HDPE diet had significant accumulations of total bile acids and different metabolism pathways such as bile acid biosynthesis, pyruvate metabolism, and carnitine synthesis. Significant enterocyte necrosis was documented in the foregut of fish fed the 2% or 8% HDPE diet; and significant cell sloughing was observed in the midgut and hindgut of fish fed the 8% HDPE diet. Fish fed the 2% HDPE diet harbored different microbiota communities compared to the control fish. This study demonstrates that HDPE ranging from 100 to 125 μm in feed can be evacuated by yellow perch with no impact on growth. However, dietary exposure to HDPE decreased whole fish nutrition quality, altered nutrient metabolism and the intestinal histopathology as well as microbiota community of yellow perch. The results indicate that extended exposure may pose a risk to fish health and jeopardize the nutrition quality of aquacultured end product. This hypothesis remains to be investigated further.

© 2022 Chinese Association of Animal Science and Veterinary Medicine. Publishing services by Elsevier B.V. on behalf of KeAi Communications Co. Ltd. This is an open access article under the CC BY-NC-ND license (<http://creativecommons.org/licenses/by-nc-nd/4.0/>).

* Corresponding author.

E-mail address: dengd@uwm.edu (D.-F. Deng).

¹ Present address: Yangtze River Fisheries Research Institute, Chinese Academy of Fishery Sciences, Wuhan 430,223, China. luxing@yfi.ac.cn

² Present address: Fisheries College, Jimei University, Xiamen, China. maying@jmu.edu.cn

³ Faculty of Agriculture, Kafrelsheikh University, Kafr El-Sheikh, Egypt. Mahmouddawood55@gmail.com

Peer review under responsibility of Chinese Association of Animal Science and Veterinary Medicine.



Production and Hosting by Elsevier on behalf of KeAi

<https://doi.org/10.1016/j.aninu.2022.01.007>

2405-6545/© 2022 Chinese Association of Animal Science and Veterinary Medicine. Publishing services by Elsevier B.V. on behalf of KeAi Communications Co. Ltd. This is an open access article under the CC BY-NC-ND license (<http://creativecommons.org/licenses/by-nc-nd/4.0/>).

1. Introduction

Microplastics (MP) are defined as plastic particles with sizes smaller than 5 mm in 1 dimension and these plastics are increasingly seen as a global environmental problem (Eerkes-Medrano et al., 2015). Based on polymer structure, MP are mainly classified as polyethylene (PE), polypropylene (PP), polystyrene (PS), polyvinyl chloride (PVC), and polyamides (PA) (Wagner et al., 2014). It is estimated that around 8 million tonnes of plastics enter the oceans every year (Gallo et al., 2018; Jambeck et al., 2015). Freshwater ecosystems are not exempt from this contamination. Over 10,000 metric tonnes of plastics end up in the Great Lakes per year coming from land-based sources including river systems, wastewater treatment plants, agricultural runoff, or surface waters of other sources (Hoffman and Hittinger, 2017; Sol et al., 2021). In addition, a growing body of research has shown that MP are present on agricultural lands (Gavigan et al., 2020; Piehl et al., 2018), which may be polluted by wastewater sludge, a soil amendment if contaminated with plastics (Frehland et al., 2020).

As emergent contaminants in aquatic systems, MP may accumulate in fish by direct ingestion from water or indirect ingestion through food web transfer (Gamarro et al., 2020; Lusher et al., 2017). Growing evidence has shown that MP accumulated in the gastrointestinal tract (GIT) of different fish species (Hunt et al., 2020; Kim et al., 2020; Kwon et al., 2020; Lusher et al., 2017; Rochman et al., 2015; Walkinshaw et al., 2020; Zhu et al., 2019). Sequeira et al. (2020) reported that among 198 species captured in 24 countries, 60% of all investigated wild capture fish and 14% of aquaculture fish contained MP in their organs. Carnivorous species accumulated more MP than omnivorous species (Sequeira et al., 2020). Based on the study by Munno et al. (2021) 8 species of fish collected from the Great Lakes accumulated MP in their GIT ranging from 3 to 915 particles/fish, with the highest abundances found in demersal fish. Over 90% of detected particles were from artificial sources and polyethylene was one of the common microplastics detected (Munno et al., 2021). These findings indicate that diverse types of food, feeding mechanisms, or habitats of different species can be reasons resulting in the different accumulation of MP.

The aquaculture industry relies on various kinds of ingredients for feed production. These include fishmeal and fish oil made from fish, terrestrial animal byproducts (feather meals, blood meals), and plant ingredients (soybean meal, corn flour, and wheat flour) from the agriculture industry and surface waters for animal production. Any pollution to the aquatic systems or the terrestrial environment could pose a risk to feed ingredients used in the aquaculture industry. For instance, high-density PE (HDPE) is one of the major MP detected in fishmeal (Thiele et al., 2021). Plastics used in aquaculture facilities (holding tanks, polyvinyl chloride (PVC) pipes, and aeration lines, and packing bags) can be the potential sources of MP contaminated in aquacultured fish. Thus, seafood generated from aquaculture systems is still vulnerable to MP contamination if no proper understanding of MP prevalence and impacts are in place for monitoring. This potential risk should be assessed to address concerns regarding fish health and the quality of aquaculture products (Mercogliano et al., 2020).

Yellow perch (*Perca flavescens*) is one of the preferred food fish and an ecologically important fish species in the Laurentian Great Lakes (Marsden and Robillard, 2004; Wilberg et al., 2005). The reduced supply of wild fish harvested has driven the development of commercial yellow perch aquaculture. While multiple factors contributed to the decline of yellow perch populations, no study to date has investigated the potential impacts of MP on this fish species. Given the concerns of MP contamination in feed ingredients and susceptibility to ingestion of MP from the surrounding environment in aquaculture settings, this study is aimed to identify potential

impacts of HDPE exposure on yellow perch. We assessed the dose–response of yellow perch exposed to HDPE based on growth performance, nutritional quality of the whole fish, liver histopathology and metabolites, and intestinal microbial community analysis. Research based on dietary exposure to aquacultured fish is still limited (Kim et al., 2020; Lyu et al., 2020). To the best of our knowledge, an integrative assessment of the risks associated with MP to aquaculture fish regarding potential impacts on nutritional quality and nutrient metabolism is still lacking. These are especially critical issues for aquaculture products regarding aquatic feed and aquaculture end product quality management besides seafood safety. The findings of the current study will help to address these gaps and provide baseline information to direct research that investigates how MP impact nutrient utilization in aquaculture fish.

2. Materials and methods

All the experimental procedures applied in this followed the animal care protocols (19-20 #50) approved by the Animal Care and Use Committee (IACUC), University of Wisconsin–Milwaukee.

2.1. Test diet preparation

High-density polyethylene (HDPE) powders with an average particle size of 125 µm was from Sigma–Aldrich (CAS#: 9002-88-4, USA). The purity of HDPE was 90.5% (Fig. 1) analyzed using Fourier Transform Infrared Spectroscopy with Attenuated Total Reflectance (FTIR-ATR). The particle size of HDPE used in this study ranged from 100 to 125 µm, which is a common size for ingredients used in aquatic feeds.

A control diet was formulated to contain 41% crude protein and 11% lipid (Table 1). Protein was provided by a combination of different ingredients including menhaden fishmeal (35%), soy protein concentrate (16%), and wheat gluten meal (8%). Additional lipid sources were obtained from fish oil (4%), corn oil (2%) and soy lecithin (1%). Five experimental diets were prepared by adding HDPE to the basal diet at a level of 0, 1, 2, 4 or 8 g/100 g dry diet at the expense of cellulose. The analytical level of HDPE were 0, 0.84, 1.57, 3.48, and 7.13 g/100 g dry diet. The highest concentration of HDPE in the test diet was below or comparable to previous studies (Alomar et al., 2021; Rochman et al., 2014), which exposed fish to test diets containing 10% MP.

All dry ingredients were pulverized to less than 400 µm particles, weighed accurately (approximately 0.1 g), and mixed into a homogeneous mash using a Hobart mixer (K5-SS, Hobart Corporation of Troy). The dry mass was blended with 40% boiled water (85 °C, wt/wt total dry mixture) and then mixed with oils before it was mixed completely to form homogeneous moist dough. The moist dough was extruded through a Hobart meat grinder to generate pellets with 3 mm diameters. The resultant moist pellets were sealed with foil, and then baked in an oven at 85 °C for 20 min to increase the gelatinization of carbohydrate and improve water stability of feed pellets. Subsequently, the feed pellets were dried at room temperature inside a laboratory fume hood (HBASC6, Lab crafters, Inc.) with blowing air until the moisture content was reduced to a level of less than 10%. The feed pellets were then crumbled and sieved to generate suitable sizes (1.5 to 3.0 mm in diameter) of pellets used for the feeding trials. All experimental diets were packed and stored at –20 °C until used.

2.2. Fish source and maintenance

Yellow perch fingerlings were produced from broodstock housed at the School of Freshwater Sciences (University of Wisconsin–Milwaukee, USA) in January 2019 and were raised until

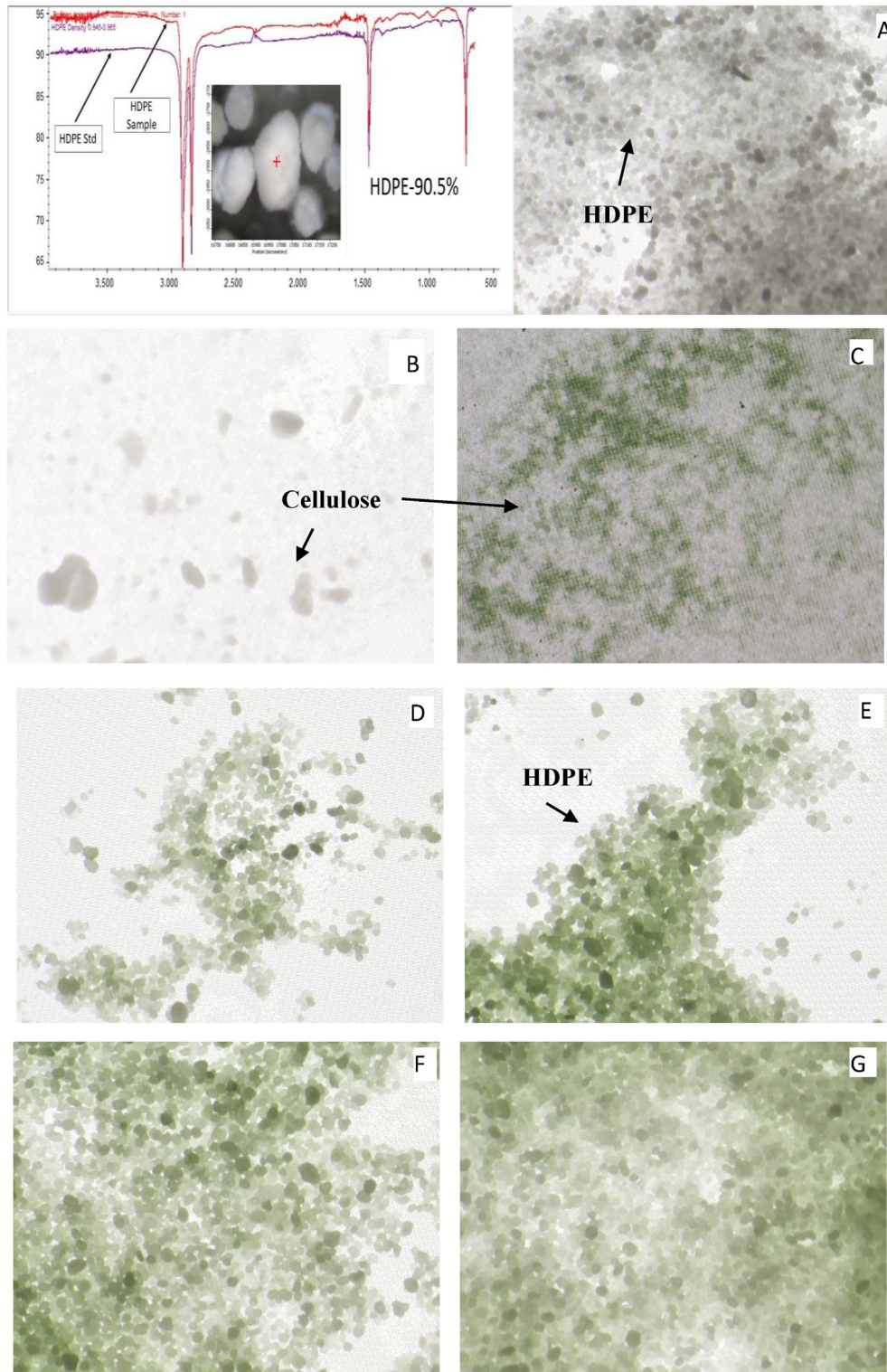


Fig. 1. Image of standard high-density polyethylene detected (HDPE), cellulose, and HDPE extracted from test diets. (A) commercial pure HDPE added to the test diets; (B) cellulose; (C) 0% HDPE diet with no added HDPE; (D) 1% HDPE; (E) 2% HDPE; (F) 4% HDPE; (G) 8% HDPE. Magnification = 32× for all pictures.

they were used for the current study. Protocols used for fish maintenance and feeding were similar to the method described by Jiang et al. (2020).

Fish were first acclimated to the culture system for 2 wk before the beginning of this feeding trial. Two hundred and seventy fish were selected and distributed into 15 tanks (100 L water) with 18 fish

per tank. The indoor culture system was run with dechlorinated municipal flow-through water at a rate of approximately 3 L/min per tank. Photoperiod was maintained at 12 h:12 h = dark:light, and the water temperature was kept at 22 °C. During the acclimation period, fish were weaned to the experimental diet gradually (0% commercial diet [42% protein and 14% lipid] for 2 d; 75% commercial diet and 25%

Table 1
Feed formulation and proximate composition of test diets containing different levels of high-density polyethylene (HDPE).

Item	Dietary HDPE, %				
	0	1	2	4	8
Ingredients, g/100 g, as fed					
Menhaden meal ¹	35.0	35.0	35.0	35.0	35.0
Soy protein concentrate ²	16.0	16.0	16.0	16.0	16.0
Wheat gluten ³	8.0	8.0	8.0	8.0	8.0
Wheat flour ³	18.0	18.0	18.0	18.0	18.0
CaHPO ₄ ·2H ₂ O ⁴	1.0	1.0	1.0	1.0	1.0
Chromic oxide ⁵	1.0	1.0	1.0	1.0	1.0
Mineral premix ³	3.0	3.0	3.0	3.0	3.0
Vitamin premix ³	2.0	2.0	2.0	2.0	2.0
Menhaden oil ³	4.0	4.0	4.0	4.0	4.0
Corn oil ⁵	2.0	2.0	2.0	2.0	2.0
Soy lecithin ⁵	1.0	1.0	1.0	1.0	1.0
Ascorbyl-palmitate ⁴	0.05	0.05	0.05	0.05	0.05
HDPE ⁴	0.0	1.0	2.0	4.0	8.0
Cellulose ⁴	8.95	7.95	6.95	4.95	0.95
Total	100.0	100.0	100.0	100.0	100.0
Proximate composition, g/100 g, as fed					
Moisture	9.8	10.3	11.1	11.3	12.3
Protein	41.5	41.2	40.7	40.8	40.8
Lipid	10.6	10.9	10.8	10.5	10.3
Ash	10.9	11.0	10.7	10.9	10.8
Sulfur	0.59	0.60	0.60	0.58	0.59
Phosphorus	1.75	1.78	1.74	1.72	1.75
Potassium	1.16	1.15	1.14	1.11	1.13
Magnesium	0.21	0.20	0.20	0.20	0.20
Calcium	2.14	2.17	2.1	2.09	2.16
Sodium	0.39	0.38	0.38	0.37	0.38
HDPE	0	0.084	1.57	3.48	7.53
Iron, mg/kg as fed	360.0	349.0	354.0	353.0	359.0
Manganese, mg/kg as fed	47.8	48.5	48.0	46.8	47.6
Copper, mg/kg as fed	8.6	9.7	10.2	8.3	9.2
Zinc, mg/kg as fed	67.9	70.6	67.7	66.5	68.4

¹ Protein Corporation, Houston, Texas, USA.

² Nelson & Sons Inc., Murray, UT, USA.

³ MP Biomedicals, Irvine, California, USA.

⁴ Sigma–Aldrich Co. St. Louis, Missouri, USA.

⁵ Alfa aesar, Tewksbury, MA 01876, USA.

control diet for 3 d; 50% commercial diet and 50% control diet for 3 d; 25% commercial diet and 75% control diet for 3 d; 100% control diet for 3 d). Fish were fed at a feeding rate of 3% total body weight 4 times daily (09:00, 11:00, 14:00 and 16:00).

At the end of the acclimation period, all fish were fasted for 24 h and then pooled into a large tank for selection and redistribution. Fish that appeared normal and similar in size (average body weight: 25.90 ± 0.16 g, $n = 15$) were randomly distributed into each tank with 15 fish per tank. Each experimental diet was randomly assigned to 3 tanks. Fish were fed using automatic feeders 4 times daily as described above and at a daily feeding rate based on body weight with 2% for the first 6 wk and 1.5% for the 7th to 9th wk. Yellow perch is very vulnerable to stress and it is difficult to achieve good growth through satiation by hand-feeding. Thus, automatic feeder was used to feed the fish based on predicted feeding rate, which were previously determined in our lab based on growth and feed conversion ratio (1.0 to 1.5; data not published). The fish were batch-weighed in water containing stress coat (1.5 mL per 10 L water; Fishcare North America, Inc., USA) every 3 wk to obtain growth data, and feeding rates were adjusted accordingly.

All tanks were cleaned by siphoning to remove fecal matter before the first feeding daily. Mortality, water temperature, pH, and dissolved oxygen were monitored daily. Total ammonia nitrogen was monitored weekly. Water temperature was maintained at 22 to 23 °C, dissolved oxygen >6.0 mg/L, ammonia nitrogen <0.08 mg/L, and pH 7.2 to 8.0. The photoperiod followed the same cycle used during acclimation period.

2.3. Sample collection

2.3.1. Whole fish for proximate composition and morphology analysis

At the end of the 9-wk feeding trial, all fish were fasted for 24 h before they were batch-weighed and counted to obtain final survival and total weight of each tank. Four individuals from each tank were randomly collected and measured for body weight and total body length, euthanized by an overdose of (0.5 g/L, Sigma–Aldrich), and kept at –80 °C until used for proximate composition analysis (moisture, crude protein, crude lipid, ash). Another 4 fish per tank were euthanized and measured for individual body weight and total length, followed by cervical severing of the spinal cord before they were dissected. These 4 fish were dissected on ice to obtain the liver, intestine, carcass and gonad for the calculations of hepatosomatic index (HSI), carcass index (CSI), and gonad index (GSI), respectively. Liver and intestine were collected for histology assessment or nutritional composition analysis as described below.

2.3.2. Liver and intestine tissues

A portion of liver tissue and gut tissues (foregut, midgut, and hindgut) from 4 fish of each tank was fixed in neutral buffered formalin (10%) at room temperature before they were processed for histopathology (Jiang et al., 2020). Another portion of liver tissue was frozen in liquid nitrogen and stored at –80 °C until used for nutrition and metabolomic analysis.

2.3.3. Whole gut sample for microbial and HDPE analysis

Three perch after 24 h of fasting were sampled from each tank following the protocol described above. The surface of each perch was wiped with 70% ethanol, and then the entire intestine (including both tissue and content) was collected with a sterilized scissors and forceps. The intestine was then wrapped in aluminum-foil, immediately frozen in liquid nitrogen, and stored at –80 °C until used for microbial analysis. Another 3 euthanized fish from each tank were dissected after 48 h of fasting to measure the length of whole GIT and total body length to calculate the ratio between the 2 lengths. The whole GIT samples were used to analyze the retention of HDPE.

2.4. Sample analysis

2.4.1. Nutrient and HDPE analysis

Proximate composition of test diets and fish samples was analyzed according to Association of Official Analytical Chemists methods (AOAC, 2000). Moisture content was determined by drying samples in a vacuum freeze dryer to reduce moisture content to a level of <10%, and then subsamples from freeze-dried samples were dried in an air-circulated oven at 105 °C for 24 h. Crude protein content was measured based on total nitrogen (total N × 6.25) levels analyzed using an elemental combustion system (ECS 4010 Nitrogen/protein analyzer, Costech Analytical Technologies, USA). Crude lipid content was determined by ether extraction using a Soxhlet Unit (Soxtec 8000 extraction unit, Foss). Ash content was measured using a muffle furnace at 550 °C for 12 h. Mineral analysis was conducted following AOAC method 985.01, and the analysis was by Midwest laboratories (Omaha, Nebraska, USA).

The concentration of HDPE in test diets, whole fish, and intestine tissue were analyzed following a method modified based on Karami et al. (2017) and Roch and Brinker (2017). Briefly, pre-weighed samples were digested in KOH (10% by weight) at 60 °C for 2 h, followed by vacuum filtration through a nylon filter membrane (30 µm). The collected sample was further digested in nitric acid (65%) at 50 °C for 15 min and then at 80 °C for 15 min.

Then deionized and distilled water was added to dilute the digestion solution (sample:water = 1:2 by volume) and then incubated at 80 °C for 30 min. The solution was cooled to room temperature before it was filtered through a 30 µm nylon membrane. The collected digestate was rinsed into 50% HDX Germicidal Bleach (8.25% sodium hypochlorite) and incubated overnight and then filtered into a pre-weighed membrane. The samples and membrane were washed with ddH₂O and then dried at 60 °C for 2 h. The weight of digestate was measured for the calculation of MP recovery. For each analysis, a sample of standard HDPE and cellulose (the same products used for feed preparation) was run simultaneously to check the recovery of HDPE. Recovered HDPE particles were examined and photographed under an Olympic microscope. Our tests showed that the recovery of HDPE with the size ranging from 100 to 125 µm was above 95%, and cellulose was completely digested using this protocol (Fig. 1).

2.4.2. Histopathological evaluation

Liver and intestine tissues previously fixed in 10% buffered formalin were processed by the Histology Core Lab at the Medical College of Wisconsin. For each sample, 3 serial sections were collected, stained with haematoxylin and eosin (H&E), and mounted on glass slides. Stained slides were digitally scanned for analyses using Nano Zoomer digital pathology system (Hamamatsu Photonics K.K.). Hepatocyte diameter and number of Kupffer cells within a 10,000 mm² area of similar location on each serial section were identified (Debofsky et al., 2018; Rašković et al., 2011). Digital measurements of hepatocyte diameters (Fig. 2) were performed using NDPview2 desktop software package (v. 2.6.13, Hamamatsu Photonics) following the same method described by Jiang et al. (2020). Specifically, the scaled linear measurement tool was used to determine hepatocyte diameter in microns. Criteria for hepatocytes identified for measurement were based on the following: 1) the hepatocyte had a clearly identifiable nucleus, and 2) a clearly defined cell margin. All cells that fit these parameters within the defined area were measured along the longest axis of the cell (Fig. 2). Kupffer cells within the same defined area were also identified.

Three portions of EACH intestine were sectioned to evaluate the microscopic anatomy and histopathology of the intestine (Fig. 3A). Image J software was used to count goblet cell numbers and measure the morphology including cross-section diameter, muscularis thickness, mucosa fold length, and villi width. The intestinal lesions were scored based on an ordinal ranking system (0 = normal to minimal, 1 = mild, 2 = moderate, and 3 = severe) using a BH-2 Olympus microscope.

2.4.3. Liver metabolite extraction and NMR spectroscopy data acquisition

Nuclear Magnetic Resonance (NMR) metabolomics analysis was used to identify potential differences in liver metabolite profiles among yellow perch fed the different diets. NMR spectroscopy is an analytical platform commonly used for metabolomic analysis since it is highly quantitative and highly reproducible, with minimal sample processing required compared to other analytical platforms, such as Mass Spectrometry (MS).

Frozen liver samples were pulverized in liquid nitrogen using Freezer/Mill (6775 model, Spex Sample Prep, Metuchen, NJ, USA). A sample aliquot of 100 mg (±3 mg) were extracted and 1D NOESY ¹H spectra were acquired following the same method described by Casu et al. (2017). The resulting spectra were processed by zero-filling to 65,536 complex points, multiplying the free induction decay (FID) by an exponential line broadening function of 0.3 Hz prior to Fourier transformation. The spectra were manually phased and the baseline was automatically corrected by applying a 5th

order polynomial. The chemical shift was calibrated by setting the standard trimethylsilylpropanoic acid (TMSP) peak at 0.00 mg/kg using Topspin 3.2 (Bruker Biospin). ¹H,¹³C heteronuclear single quantum correlation (HSQC) spectra were collected on selected samples to aid metabolite identification. In general, 2,048 data points with 128 scans and 512 increments were acquired with spectral widths of 11 mg/kg in F2 and 180 ppm in F1 (¹³C). A relaxation delay of 1.5 s and a refocusing delay corresponding to a 145 Hz ¹J_{C-H} coupling were used. The FIDs were weighted using a shifted sine-square function in both dimensions. Spectra were phased and calibrated using TopSpin 3.2.

2.4.4. DNA extraction and bacterial 16S rRNA gene sequencing of intestinal microbiota

The intestinal samples were transferred from –80 °C to thaw in an ice box for 15 min. Then the entire intestine was opened longitudinally on a sterilized glass dish cooled on ice. Any chyme or feces inside the gut was removed and cleaned with distilled water. The whole intestinal mucosa layer (including mucus) was carefully scraped using a sterile blade and immediately transferred to a 2 mL sterilized microcentrifuge tube. The intestinal mucosa was then extracted with the QIAamp Fast DNA Stool Mini Kit (catalog number, 51,604; QIAGEN, Germantown, Maryland, USA) according to the manufacturer's procedure for isolation of DNA from stools for pathogen detection. The quantity and purity of extracted DNA was assessed by a Nano-Drop Lite spectrophotometer (Thermo Fisher Scientific Inc., Waltham, MA, USA) and electrophoresis using a 1% (wt/vol) agarose gel. The variable V5–V6 region of bacterial 16S rRNA gene was amplified using the primers with 787f (5'-ATTAGAWACCCBNGTAGTCC-3'), with an illumina adapter (TCGTGGCAGCGTCAGATGTGTATAAGAGACAG) at the 5'-end and 1064r (5'-CGACRRCCATGCANCACT-3') with illumina adapter (GTCTCGTGGGCTCGGAGATGTGTATAAGAGACAG) to determine the diversity and composition of bacterial communities in the guts. All PCR reactions were performed in a reaction mixture of 25 µL, containing 12.5 µL of Kapa HiFi HotStart Ready Mix, 1.0 µL of forward and reverse primers (5 µmol/L stock), 1.0 µL of DNA extract (200 to 800 ng/µL), and 9.5 µL of nuclease-free water. The following PCR reaction was used to amplify the 16S rRNA genes: an initial denaturation at 94 °C for 5 min, followed by 30 cycles of denaturation at 94 °C for 30 s, annealing at 50 °C for 45 s, and extension at 72 °C for 60 s, and finished with a final extension at 72 °C for 5 min. Triplicate PCR reactions were run for each sample, and then the products were pooled to reduce PCR biases. The PCR performance was evaluated by running the end products on a 1.5% agarose gel. Subsequently, all quality PCR products were cleaned using Agencourt AMPure XP beads following the manufacturer's protocol (Beckman Coulter, Inc., Brea, CA, USA) before constructing a DNA library. The sample libraries were prepared according to the illumina MiSeq protocol in the Nextera XT Index kit (illumina). Indexed PCR amplicons were cleaned with AMPure beads and normalized with the SequalPrep Kit (ThermoFisher Scientific). The DNA quality and concentrations of all samples were checked using the Broad-Range Qubit 2.0 spectrophotometric assay (Thermo Fisher Scientific Inc., Waltham, MA, USA). The DNA sequencing was carried out on an illumina MiSeq with 2 × 250 chemistry at the Great Lakes Genomics Center (Milwaukee, WI, USA).

2.5. Data analysis and statistics

2.5.1. Growth performance, nutrition and fish health data analysis

Data were assessed for normality and homogeneity of variance using Shapiro–Wilks and Levene's tests, respectively, and showed no violation of these assumptions ($P > 0.05$). All results were subjected to one-way analysis of variance (ANOVA) to test the effects of

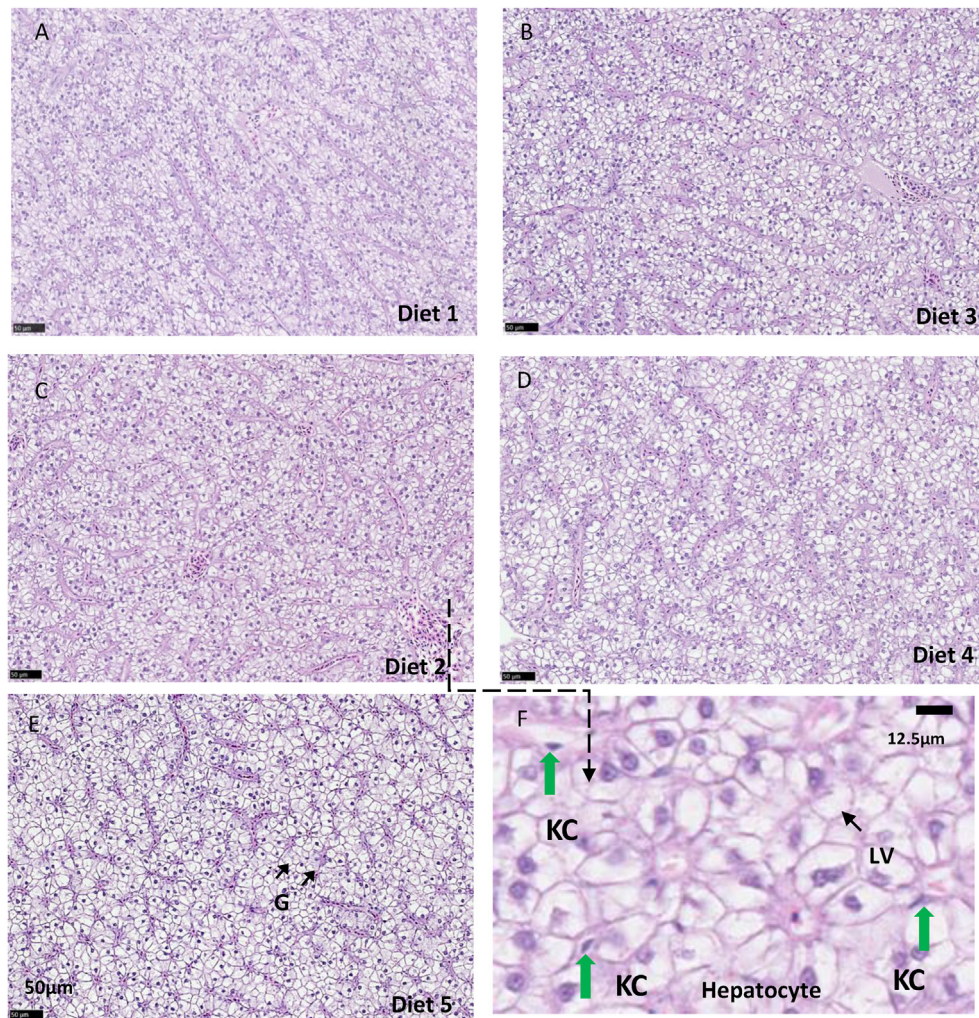


Fig. 2. Livers of yellow perch fed various test diets for 9 wk. Hepatocyte diameter and number of Kupffer cells were identified in a 10,000 mm² area of similar location on each serial section. (A) Diet 1, no added HDPE; (B) Diet 2, 1% HDPE; (C) Diet 3, 2% HDPE; (D) Diet 4, 4% HDPE; (E) Diet 5, 8% HDPE. (F) A higher magnification picture of Diet 2. G = glycogen; KC = Kupffer cell; LV = Lipid vacuoles.

different test diets on the measurements except that data on lesion score of intestines was tested using Kruskal–Wallis one-way ANOVA. The data sets were not well fitted to regression models. Thus, when significance was detected ($P < 0.05$), Duncan multiple range test was applied to identify the difference among treatments.

2.5.2. Bacterial 16S rRNA gene sequence data processing

After filtering the 16S rRNA gene sequencing data, a total of 400,756 high-quality bacterial sequences were obtained from 21 yellow perch gut mucous samples, and the average read depth was 19,083 sequences per sample. A total of 891 amplicon sequence variants (ASV) were detected across the samples. All forward and reverse reads were trimmed of their low-quality nucleotides and primers by the Great Lakes Genomic Center GNU parallel implementation of CutAdapt (Martin, 2011). The trimmed reads were then processed with the R package DADA2 (Callahan et al., 2016), following the protocol at <http://benjjneb.github.io/dada2/tutorial.html>, except that reads with a quality score lower than 10 were removed and sequences that did not have lengths (after merging) within 5% of the median sequence length were also removed. Taxonomy was assigned to the resulting unique ASV using Silva v. 132 (Quast et al., 2013). ASV not classified as bacteria were removed prior to further analyses. A negative control (extraction and PCR

blank) reaction was also sequenced. Contaminant ASV in the negative control were identified with the R package Decontam (Davis et al., 2018) and removed from all samples prior to analyses. Alpha diversity (Shannon index) and beta diversity including nonmetric multidimensional scaling (NMDS) and analysis of similarity (ANOSIM) based on Bray–Curtis distance metrics were calculated via QIIME (v1.7.0) and displayed with the R software (v2.15.3). The Duncan test and Wilcoxon test were used to examine differences in the microbial community composition and alpha diversity indexes among treatments.

2.5.3. Metabolomic data analysis

Statistically significant metabolites were identified using NMR including 1D ¹H and 2D ¹H–¹³C NMR spectra. To aid identification, chemical shifts were compared with reference spectra as well as tables noted in published reports (Nicholson et al., 1995), the Human Metabolome Database (HMDB, <http://www.hmdb.ca>) (Wishart et al., 2013), the Biological Magnetic Resonance Data Bank (BMRB, <http://bmrwisc.edu/>) (Ulrich et al., 2008), Chenomx NMR Suite profiling software (v8.1; Chenomx, Inc., Edmonton, Canada), and an in-house compiled database. Metabolite identification was achieved at a Level 2, putative identification level (Sumner et al., 2007). For multivariate statistical analysis, the spectra were binned based on the size of

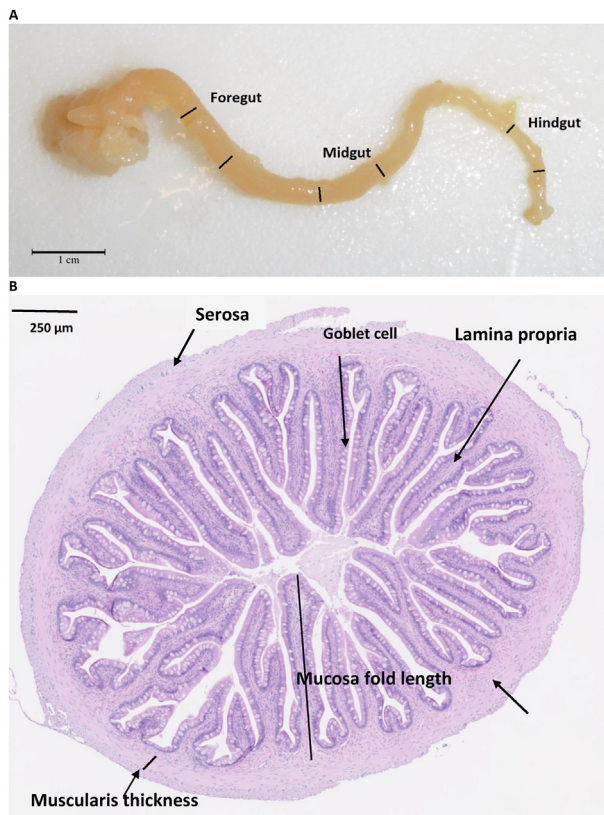


Fig. 3. (A) A whole intestine of yellow perch and (B) a cross-section of intestine for morphology measurements. Three selected portions of intestine sample (about 1 cm length) collection representing foregut, midgut, and hindgut for histology assay.

0.005 mg/kg between δ 10.0 to 0.2 mg/kg. Some spectral regions were excluded to remove artifacts due to water suppression or contaminants detected in the blank. Excluded regions include acetate (1.93 to 1.91 mg/kg), water (4.90 to 4.70 mg/kg), chloroform (7.69 to 7.67 mg/kg) and formate (8.47 to 8.45 mg/kg). Spectra were normalized to the sum of total spectral intensities and Pareto scaling was applied. Binning, scaling, and spectral alignment were performed using NMRProcFlow 1.3 software (www.nmrprocflow.org). Multivariate statistical analysis was performed using MetaboAnalyst 4.0 software (www.metaboanalyst.ca). Principal Component Analysis (PCA) followed by Partial Least Square Discriminant Analysis (PLS-DA) were performed to identify the correlation differences among different treatments with specific metabolites detected. Permutation testing was performed for PLS-DA model validation (100 random permutations). Variable Importance in Projection (VIP) scores (cut-off value of 1.5), a weighted sum of squares of partial least squares loadings, were used to select the most discriminating metabolites between the different treatments. Quantitative enrichment analysis (QEA) was performed on a set of 20 metabolites shown in the annotated spectra using the enrichment analysis module implemented in MetaboAnalyst 4.0.

3. Results

3.1. Growth performance and nutrient composition of whole fish

No mortality occurred during the feeding trial and there were no apparent signs of significant distress or adverse effects on the fish. We found no significant differences in growth performance based on percentage of weight gain (WG %), condition factor (CF), carcass

index (CSI), gonadal somatic index (GSI), and the ratio of gut length and total body length (GLR) of yellow perch by dietary exposure to HDPE for 9 wk ($P > 0.05$, Table 2). Feed conversion ratio (FCR) for fish fed the 1% HDPE diet was significantly higher than those for fish fed the control and 8% HDPE diets ($P = 0.01$). FCR was similar for fish fed the control diet and those fed the diets containing 2%, 4% or 8% HDPE ($P > 0.05$). The ratio of gut length to fish full length was not significantly different among fish fed the different test diets ($P > 0.05$). No accumulation of HDPE was detected in fish collected 24 h post-feeding and in the GIT of any fish 48 h post-feeding (data not shown).

As shown in Table 3, fish fed with 8% HDPE had significantly lower protein ($P = 0.03$) and ash content ($P \leq 0.01$) than the fish fed the diets containing 0 to 2% HDPE. The moisture and lipid contents were not significantly changed due to the exposure of HDPE ($P > 0.05$).

3.2. Morphology, nutrition composition, and antioxidative enzyme activity of liver tissue

The value of liver hepatosomatic index (HSI) significantly increased in fish fed the diets containing 2%, 4% or 8% HDPE when compared to those in fish fed the control diet ($P = 0.011$). Exposure to HDPE resulted in significant changes in the nutrient contents of the liver tissue, except for the protein content ($P < 0.05$; Table 4). The 8% HDPE diet led to a significant increase in the content of moisture and glycogen ($P = 0.04$) but decrease in lipid content ($P \leq 0.01$). Based on histological analysis, the diameter of liver cell was significantly increased in all treatments exposed to HDPE ($P = 0.01$; Table 4). Kupffer cell number was not changed and no significant lesion was observed among different treatments ($P > 0.05$). The specific activity of superoxide dismutase was not different between fish fed the control diet and the 1% HDPE diet, which significantly induced the enzyme activity of perch when compared to the diets containing 2% to 8% HDPE ($P = 0.03$).

3.3. Metabolomic analysis of liver tissue

Yellow perch fed the control diet, the 2% HDPE or 8% HDPE diets were revealed to have a high degree of similarity in representative 1D ^1H NMR spectra obtained from the liver tissue extracts (Fig. 4A).

Table 2

Effects of dietary high-density polyethylene (HDPE) exposure on growth performance and morphology of yellow perch juveniles fed the experimental diets for 9 wk¹.

Item	Dietary HDPE levels, %					Pooled SE
	0	1	2	4	8	
WG ²	202.7 ^a	210.6 ^a	202.9 ^a	210.3 ^a	203.4 ^a	2.90
FCR ³	0.98 ^b	0.93 ^a	0.95 ^{ab}	0.96 ^{ab}	0.98 ^b	0.01
CF ⁴	1.41 ^a	1.42 ^a	1.39 ^a	1.40 ^a	1.40 ^a	0.02
CSI ⁵	85.7 ^a	86.0 ^a	85.9 ^a	85.8 ^a	85.8 ^a	0.30
GSI ⁶	0.43 ^a	0.33 ^a	0.24 ^a	0.51 ^a	0.45 ^a	0.09
GLR ⁷	0.60 ^a	0.62 ^a	0.63 ^a	0.61 ^a	0.61 ^a	0.02

¹ Data were presented as mean of 3 replications. Means in the same row sharing different superscript letters are significantly different ($P < 0.05$), as determined by Duncan test.

² Weight gain (WG, %) = $100 \times (\text{Final body weight, g} - \text{Initial body weight, g}) / (\text{Initial body weight, g})$. Initial body weight was 25.9 ± 0.2 g, $n = 15$. Fish were fed with the test diet at a feeding rate of 1.5% to 2% body weight daily.

³ Feed conversion ratio (FCR) = $(\text{Dry feed weight per tank, g}) / (\text{Total weight gain per tank, g})$.

⁴ Condition factor (CF, g/cm^3) = $(\text{Body weight, g}) / (\text{Body length, cm})^3 \times 100$.

⁵ Carcass index (CSI, %) = $(\text{Carcass weight, g}) / (\text{Body weight, g}) \times 100$.

⁶ Gonadosomatic index (GSI, %) = $(\text{Gonad weight, g}) / (\text{Body weight, g}) \times 100$.

⁷ Gut and body length ratio (GLR) = $(\text{Gut length, cm}) / (\text{Body length, cm})$.

The peaks in each spectrum represent specific signals derived from all the polar metabolites with a low-molecular weight (<1,500 Da) present in each sample and are observed at specific frequencies (chemical shifts in ppm, x axis). Different classes of metabolites were detected including amino acids, carbohydrates, energy-related compounds such as tricarboxylic acid cycle intermediates and creatine, in addition to choline derivatives and bile acids. Quantitative enrichment analysis showed that the most impacted metabolic pathways included Bile Acid Biosynthesis, along with Taurine and Hypotaurine Metabolism, Pyruvate Metabolism, and Carnitine Synthesis ($P < 0.05$; Fig. 4B).

The PCA (Fig. 5A) and PLS-DA (Fig. 5B) plots based on liver NMR spectra showed that the scores were significantly separated between fish fed the control diet and the 8% HDPE diet ($P < 0.05$), while fish fed the 2% HDPE diet showed overlap scores with the other 2 treatments. PLS-DA VIP scores ranged from 1.5025 to 2.9234 for bile acids, which was significantly higher in the liver of yellow perch fed 8% HDPE than those fed the control diet ($P = 0.01$), with about 5-fold higher than the control fish (Fig. 5C). The differences between yellow perch fed 2% HDPE and those fed the control diet or the 8% HDPE diet were not statistically significant ($P > 0.05$).

3.4. Microscopic anatomy and histology of gastrointestinal tract

Similar to other teleost and vertebrate, the basic organization of intestinal structure was formed by four layers, including mucosa, sub-mucosa, muscularis, and serosa (Fig. 6A, B, and C). The foregut consists of villi (highly branched, elongated, and finger like folds) and abundance of goblet cells scattered among the simple columnar absorptive epithelia cells or enterocytes (Fig. 6D). The villi became shorter and the number of goblet cells was increased in midgut (Fig. 6E). Goblet cells became lesser in the hindgut (Fig. 6F). In general, no significant impact was observed on the morphology of midgut and hindgut of perch from different treatments ($P > 0.05$; Table 5) except that the muscularis thickness of hindgut was significantly decreased in fish exposed to 2% HDPE compared to the control fish ($P = 0.04$). The thickness remained similar between the fish fed the control diet and the 8% HDPE diet although the later tended to have a short thickness ($P < 0.05$). The average goblet cell numbers tended to decrease in the midgut of fish exposed to 2% HDPE or 8% HDPE, but no statistical difference was detected due to the large variation among samples ($P < 0.05$). The histopathology score for enterocytes necrosis was significantly higher in the foregut of fish fed the 2% HDPE or 8% HDPE diet than the scores of fish the control diet ($P = 0.01$; Table 6) but this was not different in the midgut and hindgut of perch fed with different test diets ($P > 0.05$). Cell sloughing observed in the midgut and highgut was increased in fish exposed to 8% HDPE (Table 6 and Fig. 7; $P = 0.01$) when compared to the control treatment ($P < 0.05$).

Table 3

Effects of dietary-high density polyethylene (HDPE) exposure on the nutritional compositions of yellow perch fed the experimental diets for 9 wk (% of wet whole fish).¹

Item	Dietary HDPE levels, %					Pooled SE
	0	1	2	4	8	
Moisture	68.0 ^a	67.6 ^a	67.5 ^a	67.5 ^a	67.6 ^a	0.4
Protein	16.8 ^b	16.9 ^b	16.9 ^b	16.3 ^{ab}	15.8 ^a	0.2
Ash	4.4 ^c	4.2 ^{bc}	3.9 ^{ab}	3.9 ^{ab}	3.6 ^a	0.1
Lipid	9.1 ^a	9.5 ^a	9.7 ^a	9.5 ^a	9.2 ^a	0.3

¹ Data are presented as mean of 3 replications. Means in the same line sharing different superscript letters are significantly different ($P < 0.05$) as determined by Duncan's test.

Table 4

Effects of dietary high-density polyethylene (HDPE) exposure on the liver tissue of yellow perch juveniles fed the experimental diets for 9 wk¹.

Item	Dietary HDPE levels, %					Pooled SE
	0	1	2	4	8	
HSI ² , %	1.35 ^a	1.50 ^{ab}	1.55 ^b	1.59 ^b	1.64 ^b	0.07
Hepatocyte, μm	15.6 ^a	16.6 ^b	17.2 ^b	17.2 ^b	17.0 ^b	0.34
Kupffer cell number ³	2.08 ^a	2.11 ^a	2.00 ^a	2.1 ^a	2.19 ^a	0.17
Liver, % of wet tissue						
Moisture	61.4 ^a	63.4 ^{bc}	61.8 ^{ab}	63.5 ^{bc}	63.8 ^c	0.6
Protein	9.9 ^a	10.9 ^a	10.3 ^a	10.3 ^a	10.2 ^a	0.4
Lipid	19.5 ^c	16.5 ^{ab}	18.1 ^{bc}	16.2 ^{ab}	14.9 ^a	0.6
Glycogen	8.2 ^a	8.0 ^a	8.8 ^a	9.5 ^{ab}	11.5 ^b	0.8
Enzyme activity						
SOD ⁴ , U/mg protein	51.5 ^{ab}	60.5 ^b	50.2 ^a	45.1 ^a	47.1 ^a	3.0

¹ Data are presented as mean of 3 replications. For nutritional analysis and enzyme activity evaluation; $n = 12$ for liver histological evaluation. Means within the same row sharing different superscript letters are significantly different ($P < 0.05$), as determined by Duncan's test.

² Hepatosomatic index (HSI, %) = (Liver weight, g)/(Body weight, g) $\times 100$.

³ Kupffer cell number = Number of Kupffer cells/ 10^4 mm^2 area of similar location on each serial section.

⁴ SOD = superoxide dismutase. One unit of SOD is defined as the amount of enzyme needed to exhibit 50% dismutation of the superoxide radical.

3.5. Mucous-associated microbial communities in gastrointestinal tract

As shown in Table 7, the dominant phyla were Fusobacteria (mean relative abundance, 55% to 90%), followed by Spirochaetes (5% to 20%), Proteobacteria (2% to 11%), Bacteroidetes (0.5% to 8%), and others (< 2%). The relative abundance of the intestinal dominant phyla Proteobacteria, and Bacteroidetes were significantly increased in yellow perch in the treatment of 2% HDPE ($P < 0.05$). At the family level, the Rhodobacteraceae, Saprospiraceae, Burkholderiaceae, Spirosomaceae, Crocinitomicaceae, Chitinophagaceae, Nannocystaceae and Rubritaleaceae were enriched in the fish fed the 2% HDPE diet as compared to the control and 8% HDPE diets (Fig. 8A; $P < 0.05$). *Cetobacterium* (ASV1 and ASV5, phylum Fusobacteria) was the most abundant bacterial genus and accounted for over 50% of the classified sequences across the samples. The next most prevalent sequence, ASV2 was highly abundant in many samples, but unlike ASV1, was only annotated to the family level (Spirochaetaceae, Fig. 8B). In the fish fed the 2% HDPE diet, the relative abundance of the dominant *Cetobacterium* decreased and was replaced by a large increase of a diverse array of bacteria, including *Emticia*, *Luteolibacter*, and *Limnohabitans*, among others, which led to a significantly higher Shannon index of diversity ($P < 0.05$; Fig. 9A) compared to the control or 8% HDPE groups. Although the fish fed the 2% HDPE diet harbored clearly distinct gut microbiota ($P = 0.03$) compared to the control fish, an NMDS ordination biplot also indicated that the 8% HDPE diet resulted in some samples that resembled the 2% HDPE diet microbial communities and others that were not distinguishable from the control treatment (Fig. 9B).

4. Discussion

4.1. Accumulation of HDPE in the intestine tissue or whole fish

In the current study, yellow perch were chronically fed HDPE ranging from 16.8 to 150 mg/100 g fish daily for 9 wk. This is equivalent to 4.5 to 36 mg of HDPE per meal for 100 g fish. Our results demonstrate that juvenile yellow perch were able to

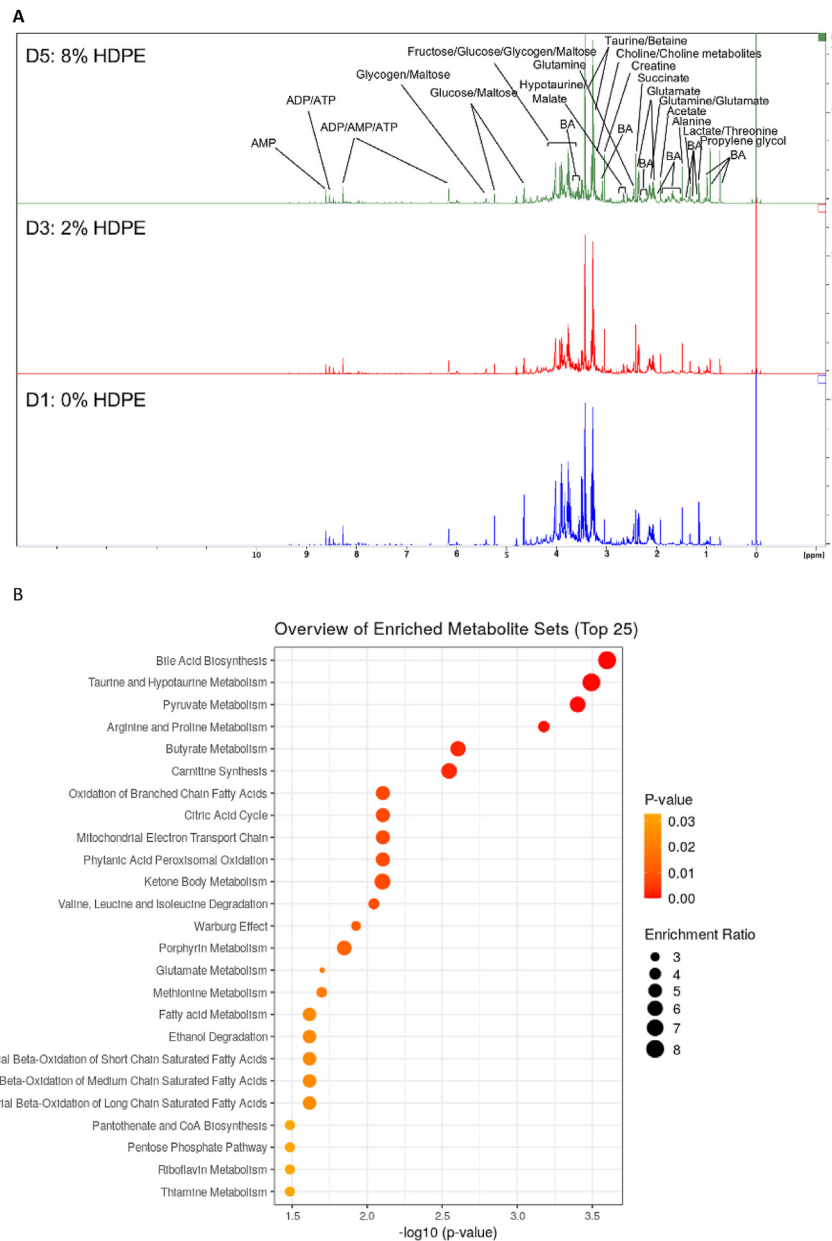


Fig. 4. (A) 1D ^1H Nuclear Magnetic Resonance (NMR) spectra recorded using a 700 MHz NMR spectrometer on polar liver extracts of yellow perch fed diet 1 (D1), diet 3 (D3), and diet 5 (D5) for 9 wk. Identified metabolites are annotated. (B) Summary plot for Quantitative Enrichment Analysis (QEA) based on a list of 20 metabolites detected by NMR in yellow perch liver extracts. BA = bile acids; HDPE = high-density polyethylene.

evacuate HDPE (100 to 125 μm) efficiently under the culture conditions because no HDPE was detected in the gastrointestinal tract or the whole fish after fasting for 24 to 48 h. It is possible that the molecular weight of HDPE is too high to penetrate through cell membranes and its particle size (100 to 125 μm) is too large to be translocated across the GIT. This hypothesis agrees with the suggestion by Kim et al. (2021) that the size of MP particles, rather than exposure routes and environmental conditions, influence the extent of accumulation.

The translocation of MP from the GIT to other tissues of fish has been reported but different results were demonstrated across studies. Critchell and Hoogenboom (2018) demonstrated that the accumulation of MP in GIT and its impact on fish growth was size-

dependent. Similar to our findings, Grigorakis et al. (2017) stated that MP ranging from 50 to 500 μm did not accumulate over succeeding meals in goldfish (*Carassius auratus*). A recent study by Kim et al. (2020) showed that spherical MP (10 to 300 μm) of PE could be effectively excreted by adult rainbow trout (*Oncorhynchus mykiss*) without translocation to other tissues. In contrast, Barboza et al. (2020) reported that MP were present in tissues, including muscle and gills of fish captured in coastal waters. Avio et al. (2015) detected MP (200 to 600 μm) accumulation in the liver tissue of flathead grey mullet (*Mugil cephalus*) under laboratory testing conditions. Similarly, MP with sizes up to 250 μm were found in the liver of fish collected from the Persian Gulf (Abbasi et al., 2018). Given the large size of those MP, De

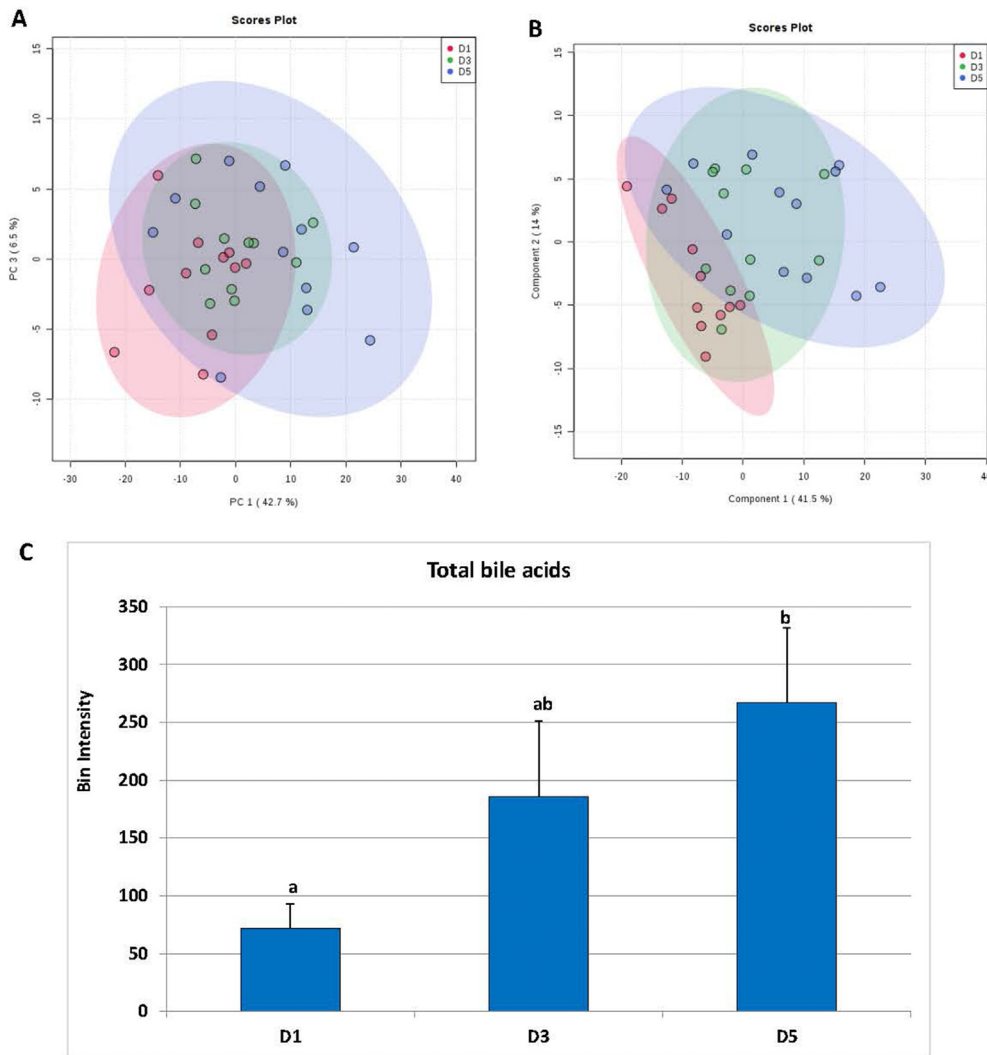


Fig. 5. (A) Principal Component Analysis and (B) Partial Least Square Discriminant Analysis (PLS-DA) score plots derived from Nuclear Magnetic Resonance (NMR) spectra of liver extracts from yellow perch fed D1 (0% HDPE), D3 (2% HDPE) or D5 (8% HDPE) for 9 wk. Circles represent individual liver samples and NMR spectra. Shaded areas represent the 95% confidence regions for each group. Permutation testing ($n = 100$, $P = 0.02$) was performed for PLS-DA model validation. (C). Relative levels of total bile acids in liver extracts of yellow perch fed D1, D3, or D5 for 9 wk. P -values were calculated using a t -test (letters of a and b indicated statistical significance at $P < 0.05$ among treatment). HDPE = high-density polyethylene.

Sales-Ribeiro et al. (2020) and Jovanović et al. (2018) raised questions on the plausibility of these findings and expressed concerns on the possibility of cross-contamination. On the other hand, the potential of translocation and accumulation of smaller size MP were found in aquatic organisms. Lu et al. (2016) found that 5 μm polystyrene accumulated in the liver tissue of zebrafish (*Denio rerio*). Similarly, De Sales-Ribeiro et al. (2020) observed MP (up to 1.6 μm) in the liver tissues of adult zebrafish. These findings indicate that smaller particles potentially have greater health impacts and may have long-term biological effects if accumulated. In our study, a larger HDPE size (100 to 125 μm) was selected because it is relevant to the size of feed ingredients commonly used in aquaculture for juvenile or grow-out fish. The findings in this study do not exclude the potential of MP translocation through the GIT or the accumulation of MP in yellow perch if smaller sizes or different types of MP were exposed to the fish for a longer time. Furthermore, MP retention times and excretion rates from the GIT may be dependent on the shape and type of MP ingested as discussed by Smith et al. (2018). These issues should be addressed in future research.

4.2. Impact on the growth performance and nutrition composition of whole fish

MP pollution has been reported to cause different impacts on aquatic organisms including alteration of gene expression, increased cellular inflammation, interruption of tissue integrity, disruption in energy metabolism and immunity, retarded growth, and decreased reproductive performance (Critchell and Hoogenboom, 2018; Gardon et al., 2020; Karami et al., 2017; Rochman et al., 2014; Sussarellu et al., 2016; Lu et al., 2016). Different effects of MP have been reported across studies dependent on the exposure routes, species of fish, the types and sizes of MP, and the parameters used for monitoring. Our results showed that the exposure of HDPE at 100 to 125 μm sizes did not adversely influence the growth and survival of yellow perch but did cause significant impacts on nutrient metabolism. The overall growth rate of yellow perch in the current study was similar to our previous studies (Jiang et al., 2019; 2020). Thus the fish were maintained in their normal growth rate during this 9-wk exposure trial. The finding was similar to those observed in other fish species. Through

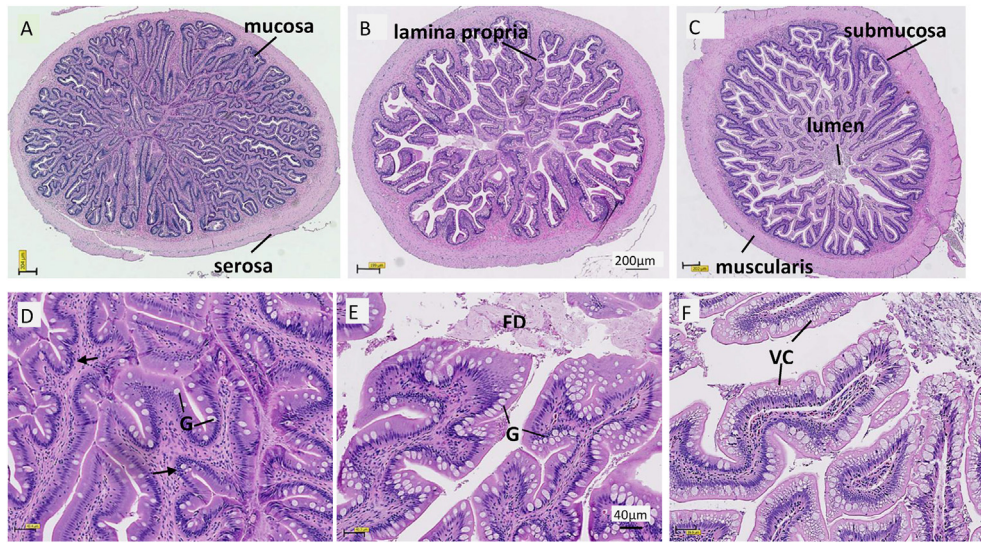


Fig. 6. Gastrointestinal tracts of yellow perch fed control diet showing (A) foregut, (B) midgut, and (C) hindgut of yellow perch. Scale bar = 200 μ m. (D) Higher magnification of foregut showing the mucosa layer of foregut with highly branched, elongated, and finger like villi (arrows) and few goblet cells scattered among the enterocytes. Scale bar = 40 μ m. (E) Higher magnification of midgut showing flatter villi with large number of goblet cells in the midgut. Scale bar = 40 μ m. (F) Higher magnification of hindgut showing reduction in goblet cells and increase in vacuolated enterocytes (VC) in the hindgut. Scale bar = 40 μ m. FD = food in the lumen.

Table 5
Effects of high-density polyethylene (HDPE) exposure on the intestinal morphology of yellow perch juveniles fed experimental diets for 9 wk¹.

Item	Dietary HDPE levels, %			Pooled SE
	0	2	8	
Midgut				
Cross section diameter, mm	2.19	2.09	1.95	0.19
Muscularis thickness, mm	0.14	0.13	0.11	0.02
Cross section inner area, mm ²	2.95	2.57	2.40	0.52
Villi area, mm ²	2.25	1.95	2.01	0.44
Mucosa fold length, mm	0.50	0.52	0.57	0.05
Villi width, mm	0.11	0.11	0.10	0.01
Goblet cell number	2,147	1,677	1,498	301
Hindgut				
Cross section diameter, mm	2.71	2.51	2.56	0.13
Muscularis thickness, mm	0.30 ^b	0.21 ^a	0.25 ^{ab}	0.02
Cross section inner area, mm ²	3.84	3.16	3.27	0.37
Villi area, mm ²	3.01	2.58	2.50	0.30
Mucosa fold length, mm	0.68	0.62	0.64	0.07
Villi width, mm	0.11	0.11	0.12	0.01

¹ Data are presented as mean of nine fish from 3 replications per treatment. Means within the same row sharing different superscript letters are significantly different ($P < 0.05$), as determined by Duncan's test.

Table 6
Histopathology evaluation of intestine from yellow perch juveniles fed the experimental diets with different levels of high-density polyethylene (HDPE) for 9 wk¹.

Item	Dietary HDPE levels, %		
	0	2	8
Foregut			
Necrosis of enterocytes	0.22 ± 0.15 ^a	1.44 ± 0.24 ^b	1.33 ± 0.17 ^b
Cell sloughing	0.11 ± 0.11 ^a	0.56 ± 0.18 ^a	0.67 ± 0.24 ^a
Midgut			
Necrosis of enterocytes	0.00 ± 0.00 ^a	0.67 ± 0.17 ^b ^a	0.67 ± 0.24 ^a
Cell Sloughing	0.00 ± 0.00 ^a	0.22 ± 0.22 ^a	0.89 ± 0.11 ^b
Hindgut			
Necrosis of enterocytes	0.00 ± 0.00 ^a	0.22 ± 0.15 ^a	0.00 ± 0.00 ^a
Cell sloughing	1.11 ± 0.26 ^a	1.56 ± 0.18 ^{ab}	2.44 ± 0.29 ^b

¹ Data are presented as mean of nine fish per treatment. Means within the same row sharing different superscript letters are significantly different ($P < 0.05$) as determined by Duncan's test. Lesion score was ranked as: 0 = normal to minimal, 1 = mild, 2 = moderate, and 3 = severe.

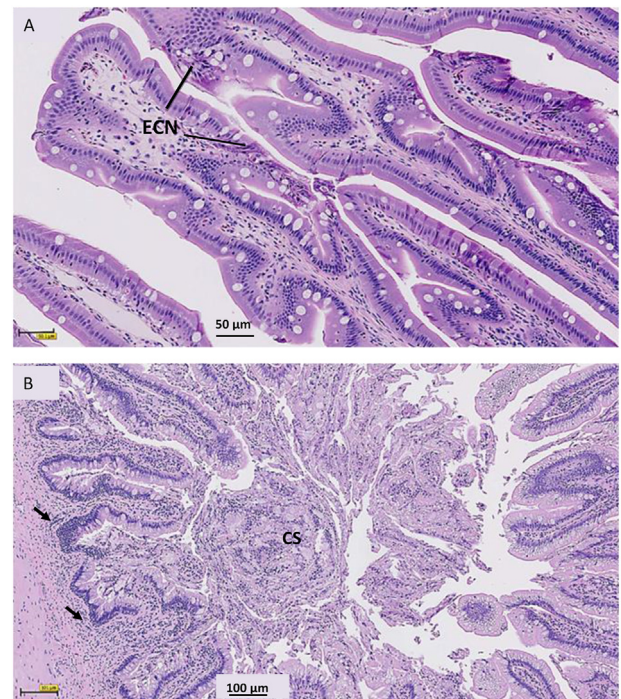


Fig. 7. Gastrointestinal tracts of Yellow Perch fed 8% HDPE diet showing (A) moderate to severe necrosis of enterocytes (ECN) in the foregut (scale bar = 50 μ m) and (B) severe infiltration of inflammatory cells (arrows) and cell sloughing (CS) in the hindgut (scale bar = 100 μ m).

a 3-month dietary exposure study, Alomar et al. (2021) reported no negative impact of low-density polyethylene MP on the growth of gilthead bream (*Sparus aurata*). Wen et al. (2018) showed that chronic exposure to MP (polyethylene) did not alter survival and growth of juvenile Amazonian cichlid (*Symphysodon aequifasciatus*), but significantly changed the activities of enzymes involved in digestion and energy metabolism. Zeytin et al. (2020) observed that European seabass (*Dicentrarchus labrax*) exposed to MP for 16 wk

Table 7

Relative abundances of the bacterial phyla in the intestine of yellow perch fed the experimental diets with different levels of high-density polyethylene (HDPE) for 9 wk.¹

Item	Dietary HDPE levels, %		
	0	2	8
Fusobacteria	89.49 ± 9.34	55.59 ± 27.30	83.02 ± 12.31
Spirochaetes	5.66 ± 6.34	20.89 ± 11.70	10.80 ± 8.69
Proteobacteria	1.88 ± 1.43 ^b	10.84 ± 6.11 ^a	3.75 ± 2.78 ^b
Bacteroidetes	0.62 ± 0.89 ^b	8.06 ± 7.07 ^a	0.81 ± 0.88 ^b
Actinobacteria	1.28 ± 2.42	0.48 ± 0.44	0.45 ± 0.63
Patescibacteria	0.50 ± 0.55	0.27 ± 0.18	0.52 ± 0.62
Verrucomicrobia	0.04 ± 0.05 ^b	0.87 ± 0.70 ^a	0.04 ± 0.60 ^b
Nitrospirae	0.00 ± 0.00	0.77 ± 1.08	0.00 ± 0.00
Planctomycetes	0.05 ± 0.08 ^b	0.61 ± 0.78 ^a	0.10 ± 0.13 ^b
Firmicutes	0.35 ± 0.69	0.14 ± 0.14	0.28 ± 0.39
Gemmatimonadetes	0.00 ± 0.00	0.52 ± 0.83	0.03 ± 0.06
Acidobacteria	0.00 ± 0.00 ^b	0.33 ± 0.24 ^a	0.03 ± 0.03 ^b
Deinococcus_Thermus	0.00 ± 0.00	0.28 ± 0.20	0.02 ± 0.05
Chloroflexi	0.00 ± 0.00	0.23 ± 0.19	0.03 ± 0.05
Unclassified	0.07 ± 0.09	0.05 ± 0.05	0.09 ± 0.07
Chlamydiae	0.02 ± 0.03	0.04 ± 0.06	0.04 ± 0.03
Cyanobacteria	0.02 ± 0.03	0.01 ± 0.03	0.01 ± 0.01
Tenericutes	0.01 ± 0.03	0.01 ± 0.02	0.00 ± 0.00
Dependentiae	0.01 ± 0.02	0.00 ± 0.00	0.01 ± 0.02
WPS_2	0.00 ± 0.00	0.01 ± 0.01	0.00 ± 0.00

¹ Values are presented as means ± standard deviation ($n = 6$ for treatment with no HDPE; $n = 8$ for treatment with 2% HDPE; $n = 7$ for treatment with 8% HDPE). Means in the same row with different superscripts are significantly different by Wilcoxon test ($P < 0.05$).

had similar growth compared to the control fish even though MP particles were detected in the fillet. These findings suggested that among different biological impacts, fish growth and survival may not be sensitive biomarkers reflecting the impact of MP. Other measurements may be needed to provide early warning related to the impact of MP.

In the present study, we observed a lower FCR for the feed containing 1% HDPE compared to the control diet and 8% HDPE diet. The different FCR seems to relate to the good water stability and density of feed pellets for the 1% HDPE diet. With the increasing level of HDPE in the test diets, water stability based on dry matter retention (20 min-duration testing) was 92.6%, 95.5%, 94.5%, 94.5% and 93.0%, and density was 487, 464, 451, 423, 430 g/L. The 1% HDPE diet has the highest water stability, but the control diet and the diet 8% HDPE had the lowest water stability. The density of diet 1%HDPE allowed feed pellets to sink slowly, which are preferred by perch. Thus, the difference in physical quality of pellets may attribute to the low FCR of fish fed the 1% HDPE diet. With the feeding strategy of this study, the overall FCR of each diet was low and we did not observe excess feed pellets during the feeding trial. Thus, it is unlikely that the fish from treatments with a higher FCR (control and 8% HDPE groups) were overfed. In addition, the actual feed intake was not measured and the FCR was based on total feed fed/weight gain in this study. The conclusion based on the FCR should consider this limitation. This result also suggests that the physical quality of feed pellets should be taken into consideration in future studies that involve dietary exposure of MP to aquatic organisms, which have different feeding habits.

Proximate composition analysis serves as an indicator of the overall nutritional and physiological condition of a fish (Ali et al., 2005). The decrease in protein and ash contents indicated that nutrient utilization was impaired in these fish although the exact reasons remained to be investigated. In the current study, all test diets were formulated to contain an equal level of protein (and amino acids) and gross energy, and they were fed to the fish at the same feeding rate based on body weight (%) daily. Furthermore, no rejection of feeding was observed during feeding. Thus, feed intake

may not be the major factor responsible for the reduced protein and ash in the fish espoused to HDPE. However, whether the digestion and absorption processes of yellow perch were disrupted by HDPE was unknown due to lacking information on the nutrient digestibility of test diets. Based on previous findings by Wen et al. (2018), PE microplastic adversely influenced digestion capacity of an Amazonian cichlid and thus reduce dietary amino acid utilization. In addition, a high level of dietary exposure to HDPE might lead to reduced protein synthesis or increased protein degradation (catabolism) for energy or other physiological functions. This is partially supported by the Metabolomic analysis (discussed below), which showed alternation of a series of metabolism processes in the liver tissues of fish when compared to the control and the 8% HDPE groups. This reduction or degradation of protein might be further exacerbated by increased infiltration of inflammatory cells, enterocyte cell necrosis, and sloughing in the gastrointestinal tract in fish exposed to HDPE.

4.3. Alteration of liver metabolism and histology

Metabolomics has emerged as a way to obtain comprehensive metabolite profiles, which enables biomarker discovery in response to treatments. With this approach, we observed significantly higher levels of bile acids in the liver tissue of perch fed the 8% HDPE diet when compared with the control fish. The increased levels of bile acids are likely due to the increased synthesis and/or reduced excretion of bile acids from the liver tissues. Yellow perch might increase bile acids synthesis to deal with HDPE, which is a polymeric material that has hydrophobic properties like lipid. This is supported by the Quantitative Enrichment Analysis, which demonstrated that Bile Acid Synthesis and Taurine and hypotaurine metabolism were significantly changed in response to HDPE exposure. In addition, bile acids production is generally high during postprandial stages in comparison with the fasting state. The high concentration of bile acids might relate to the extended food transit time in the intestine of perch fed 8% HDPE, which could delay digestion or clearance rate of digesta. In this regard, feed transition time should be determined in a future study to confirm this hypothesis. A recent study by Jiang et al. (2021) observed similar growth of mice between the control and polystyrene MP exposure mice, but an increased level of bile acids was documented in liver tissues, while with decreased levels in feces and blood circulation. Based on gene expression analysis, the study suggested that the increase of bile acids in the liver was due to the induced synthesis and decreased excretion of bile acids in the MP exposed mice. The response of bile acids level observed in our study might share a similar mechanism observed by Jiang et al. (2021), but this hypothesis will need to be investigated with further study.

The reduced level of liver lipid documented for fish fed 8% HDPE might relate to increased use of cholesterol, which is required for bile acid synthesis (Hofmann, 1999). In addition, the alteration of fatty acid metabolism and carnitine synthesis as demonstrated by the Enrichment Analysis might also explain the decreased lipid level observed in the liver tissues of HDPE-exposed fish. Furthermore, bile acids are recognized as hormone-like signaling molecules that are involved in the regulation of different metabolic processes such as glucose and energy homeostasis (Houten et al., 2006; Lefebvre et al., 2009). As signaling molecules, bile acids have been demonstrated to bind with farnesoid X receptor in liver tissue to modulate postprandial glucose levels through decreasing liver gluconeogenesis accompanied by induction of hepatic glycogen synthesis (Shapiro et al., 2018; Zhang et al., 2006). Thus, the increased level of bile acids might be one of the reasons leading to the increased glycogen level in the perch fed the 8% HDPE diet. Furthermore, the change of pyruvate metabolism in response to

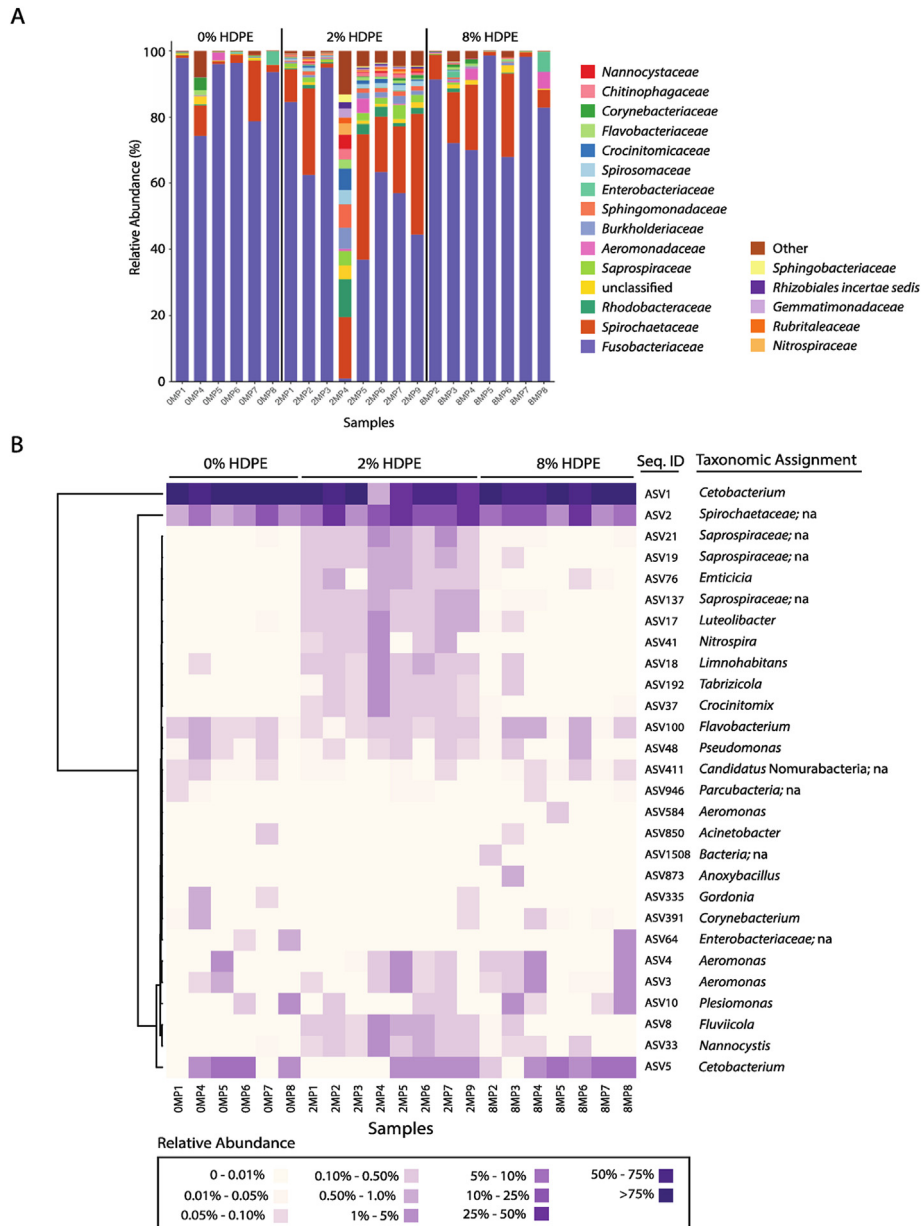


Fig. 8. (A) Stacked bar plot of bacterial relative abundance at the family-level of taxonomic assignment, and (B) a heatmap of the top 5 most abundant amplicon sequence variants (ASV) in each sample across all samples. ASV clustering by relative abundance pattern is displayed with a dendrogram and the most refined taxonomic classification is listed. Yellow perch fed diets containing 0%, 2%, or 8% of HDPE 9 wk. HDPE = high-density polyethylene.

HDPE might induce glycogenesis, which could attribute to the accumulated glycogen observed in perch exposed to HDPE.

While no adverse liver histopathology was observed in fish exposed to HDPE, we observed larger glycogen-rich hepatocytes, increased liver weight, and hepatosomatic index in fish exposed to the highest dose of HDPE. An elevated level of glycogen is normally hydrated with water, resulting in increased moisture content, and decreased lipid levels. Consequently, an increase in liver weight and the hepatosomatic index was observed in these fish. Furthermore, as an important antioxidant defense against oxidative stress, superoxide dismutase (SOD) did not show dose-responsive to the dietary levels of HDPE. The enzyme activity tended to increase in perch exposed to the 1% HDPE compared to the control fish although no statistical difference was detected due to large

variation of measurements. The activity was significantly higher in fish fed the 1% HDPE diet than those fed the diets containing HDPE from 2% to 8%. Exposure to HDPE might cause oxidative stress, leading to an activation of antioxidant responses and thus increased antioxidant activity was observed. On the other hand, a higher-level exposure to HDPE might overwhelm the defense system because combating oxidative stress requires energy (Hamed et al., 2020). This finding is similar to the observation on Chinese mitten crab (*Eriocheir sinensis*), with increased SOD activity when exposed to low concentrations (40 and 400 µg/L) of microplastic and decreased activity when the crab was exposed to higher concentrations (4,000 and 40,000 µg/L) (Yu et al., 2018). With the limited observation and the large variation results in our study, this observation needs to be confirmed in the future study.

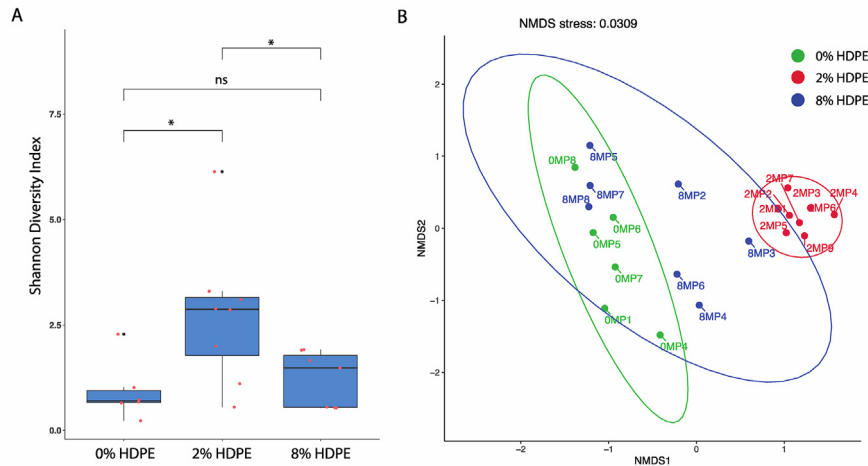


Fig. 9. (A) Box plot of the bacterial community alpha diversity (Shannon index). All measurements are indicated as points, and the box plot indicates median, and the 1st and 3rd quartiles within each diet group. Significant differences ($P \leq 0.05$) among diet groups is indicated with an asterisk and ns = not significantly different (Wilcoxon rank sum test). (B) Non-metric multidimensional scaling plot, NMDS of bacterial community beta diversity among diet treatments. Ellipses contain all samples in a given diet condition. Yellow perch fed diets containing 0%, 2%, or 8% of HDPE 9 wk. HDPE = high-density polyethylene.

4.4. Alteration of intestinal histology and microbiota

Different impacts on intestine tissues due to MP exposure have been reported previously such as gut mucosal damage occurred in Japanese medaka (*Oryzias latipes*), intestine inflammation in goldfish (*Carassius auratus*), and damaged distal intestine in sea bass (*Dicentrarchus labrax*) (Jabeen et al., 2018; Pedà et al., 2016; Zhu et al., 2019). The impacts varied depending on the species of fish, the type and size of MP applied in a study. In the current study, induced necrosis and cell sloughing or shredding of enterocytes from perch exposed to HDPE, indicating that intestinal functions of the fish were altered. The frontgut seems to have more impairment than the rest parts of the GIT. A long term stress to these fish by HDPE exposure may lead to impaired fish health because exceeding epithelial cell sloughing may cause epithelial injury. Furthermore, necrosis represents an unregulated cell death and is a passive process, which may result in a breakdown of the intestinal barrier of cell membrane and thus subsequent release of cellular compounds into the extracellular space and inflammation (Negroni et al., 2015). Thus, intestinal microbiota community, nutrient digestion and absorption could occur due to enterocyte necrosis.

In this study, *Fusobacteria*, particularly classified to the genus *Cetobacterium* and an unclassified Spirochaetaceae were the dominant bacteria inhabiting the yellow perch intestines. Other recent studies of various perch species have identified several microorganisms classified to a number of different phyla, including Proteobacteria, Bacteroidetes, Tenericutes, Firmicutes, *Fusobacteria*, and Actinobacteria as being common in perch guts. So far, the composition of the dominant bacteria seems to vary among perch species and is related to host selection, habitat, diet, and external perturbations (Cheaib et al., 2020; Tarnecki et al., 2017; Zha et al. (2018); Zhang et al., 2020), but with relatively little known about perch microbiota, no consistent drivers of gut microbial composition have emerged. In the only other study on yellow perch, a markedly different microbial intestinal composition was identified, including more dominant community members classified as Tenericutes, Firmicutes, and Euryarchaeota (Cheaib et al., 2021), but the differences in rearing conditions, diet, and 16S rRNA gene methodology make it difficult to draw conclusions between that study and the present one.

The MP diet perturbation had a significant impact on the yellow perch gut microbiota. Unexpectedly, changes in the community composition were the greatest at a 2% rather than 8% HDPE exposure, even though both diets harbored fish gut bacterial communities that were altered from the control samples, which were fairly consistent. One possibility is that the complete replacement of cellulose by HDPE in the 8% HDPE diet limited the growth of microbes not already established in the gut at the time of the perturbation. In contrast, the 2% HDPE fish had the combination of a gut perturbation (the MP) but with only partial replacement of the cellulose, which allowed for rarer members to take advantage of the community disturbance and available food to grow to higher densities. The other possibility is that fish exposed to the higher dose of HDPE responded by the increased infiltration of immune cells and cell sloughing which may affect the survival and growth of microbes. Other perch studies examining interactions between diet and microbiota have also found that *Fusobacteria* are significantly reduced in the gut during diet perturbations, such as when the food ration was altered (Zha et al. (2018)) or corn starch was supplemented (Zhang et al., 2020). This may suggest that there is a strong link between *Fusobacteria* and a healthy gut ecosystem in perch that can be altered by diet perturbations. The MP perturbation had clear physiological effects involving the liver and fish nutrient status. It is not clear if the responses were associated with the changes in gut microbiota; however, our results suggest this connection is possible and should be investigated further. In other model fish systems, such as the adult zebrafish (Jin et al., 2018) and juvenile guppy (Huang et al., 2020), MP have been found to induce microbiota dysbiosis and tissue inflammation. We also observed a change in the microbiota in response to HDPE in the diet, but it is not clear whether this was a factor or response to physiological metabolism disorder in these yellow perch. More work on identifying changes in the microbiota–host interactions and transfer of bioactive molecules during MP accumulation in fish guts is needed to tease apart the effects of this pollutant on fish in an aquaculture setting.

5. Conclusions

The results of this study demonstrate that yellow perch do not accumulate the HDPE of 100 to 125 μm in their body after 9-wk

dietary exposure. Chronic exposure had no significant impact on the growth and survival of perch but the nutritional quality of fish are downgraded with less protein and ash content in the exposed fish. Exposure to HDPE significantly change nutrient metabolism involved bile acid biosynthesis, carnitine synthesis, and pyruvate metabolism of yellow perch, and disrupte intestinal histopathology and microbiota diversity. As such, our results indicate that it is likely a long period of exposure to the MP may lead to impaired nutrient utilization and fish health. This hypothesis requires further investigation. Furthermore, the impact by which MP interfere with feed intake and its transition time through GIT, nutrient digestion and absorption remains to be elucidated in this species and warrants future study.

Author contributions

Xing Lu involved in conceptualization, experimental design and feeding trial performance, and manuscript preparation. **Dong-Fang Deng** conceptualized and administrated the project, involved in data curation and manuscript writing. **Fei Huang** and **Ryan Newton** involved in experimental design, sample collection, microbiota analysis and data interpretation. **Fabio Casu** and **Aaron M. Watson** were responsible for liver metabolomic analysis and data interpretation. Emma Kraco involved in the feeding trial performance, sample collection and analysis. **Merry Zohn** performed analysis of microplastic and liver enzyme activity. **Swae J. Teh**, **Brian Shepherd**, and **Mahmound Abdelhamid Omran Dawood** involved in histopathology evaluation, data collection and interpretation. **Ying Ma** involved in experimental design, feeding trial management, and sample collection. **Lorena M. Rios Mendoza** involved in analysis of microplastic analysis and conceptualization. All authors involved in the preparation of this manuscript.

Declaration of competing interest

We declare that we have no financial and personal relationships with other people or organizations that can inappropriately influence our work, and there is no professional or other personal interest of any nature or kind in any product, service and/or company that could be construed as influencing the content of this paper.

Acknowledgements

The current study was partially funded by the University of Wisconsin-Milwaukee (UWM, Project 150-25-3150-343 PRJ93WQ) and USDA-ARS in-house project #s 5090-31320-004-00D and 5090-31320-005-00D. UW-system water research fellowship and UWM SURF were supported to Emma K. Kraco. Naulin Foundation was awarded to Deng's lab to support part of the study. Merry Zohn was supported by fellowship with the Oak Ridge Institute for Science Education. Xing Lu (201803260002) and Fei Huang (201806330033) were supported by the China Scholarship Council. Ying Ma was supported by the Education Department of Fujian Province, China. Mahmoud A.O. Dawood was a fellow supported by USAID in Egypt. The authors wish to thank Peter Shep, Xiao jin Xu, and Huihong Zhao for their assistance during sampling.

References

Abbasi S, Soltani N, Keshavarzi B, Moore F, Turner A, Hassanaghaei M. Microplastics in different tissues of fish and prawn from the Musa Estuary, Persian Gulf. *Chemosphere* 2018;205:80–7.

- Ali MZ, Jauncey K. Approaches to optimizing dietary protein to energy ratio for African catfish *Clarias gariepinus* (Burchell, 1822). *Aquacult Nutr* 2005;11(2): 95–101.
- Alomar C, Sanz-Martín M, Compa M, Rios-Fuster B, Álvarez E, Ripolles V, Valencia JM, Deudero S. Microplastic ingestion in reared aquaculture fish: biological responses to low-density polyethylene controlled diets in *Sparus aurata*. *Environ Pollut* 2021;280:116960.
- AOAC. Official methods of analysis. 17th ed. Washington DC: AOAC International; 2000.
- Avio CG, Gorbi S, Regoli F. Experimental development of a new protocol for extraction and characterization of microplastics in fish tissues: first observations in commercial species from Adriatic Sea. *Mar Environ Res* 2015;111: 18–26.
- Barboza LGA, Cunha SC, Monteiro C, Fernandes JO, Guilhermino L. Bisphenol A and its analogs in muscle and liver of fish from the North East Atlantic Ocean in relation to microplastic contamination. Exposure and risk to human consumers. *J Hazard Mater* 2020;393:122419.
- Callahan BJ, McMurdie PJ, Rosen MJ, Han AW, Johnson AJA, Holmes SP. DADA2: high-resolution sample inference from Illumina amplicon data. *Nat Methods* 2016;13:581–3.
- Casu F, Watson AM, Yost J, Leffler JW, Gaylord TG, Barrows FT, Sandifer PA, Denson MR, Bearden DW. Metabolomics analysis of effects of commercial soy-based protein products in red drum (*Sciaenops ocellatus*). *J Proteome Res* 2017;16(7):2481–94.
- Cheabib B, Seghouani H, Ijaz UZ, Derome N. Community recovery dynamics in yellow perch microbiome after gradual and constant metallic perturbations. *Microbiome* 2020;8(1):1–19.
- Cheabib B, Seghouani H, Llewellyn M, Vandal-Lenghan K, Mercier PL, Derome N. The yellow perch (*Perca flavescens*) microbiome revealed resistance to colonisation mostly associated with neutralism driven by rare taxa under cadmium disturbance. *Anim Microbiome* 2021;3(1):1–19.
- Critchell K, Hoogenboom MO. Effects of microplastic exposure on the body condition and behaviour of planktivorous reef fish (*Acanthochromis polyacanthus*). *PLoS One* 2018;13(3):e0193308.
- Davis NM, Proctor DM, Holmes SP, Relman DA, Callahan BJ. Simple statistical identification and removal of contaminant sequences in marker-gene and metagenomics data. *Microbiome* 2018;6:226.
- De Sales-Ribeiro C, Brito-Casillas Y, Fernandez A, Caballero MJ. An end to the controversy over the microscopic detection and effects of pristine microplastics in fish organs. *Sci Rep* 2020;10:12434.
- Debofsky AR, Klingler RH, Mora-Zamorano FX, Walz M, Shepherd B, Larson JK, Anderson D, Yang LB, Goetz F, Basu N, Head J, Tonellato P, Armstrong BM, Murphy C, Carvan MJ. Female reproductive impacts of dietary methylmercury in yellow perch (*Perca flavescens*) and zebrafish (*Danio rerio*). *Chemosphere* 2018;195:301–11.
- Eerkes-Medrano D, ThoMPon RC, Aldridge DC. Microplastics in freshwater systems: a review of the emerging threats, identification of knowledge gaps and prioritisation of research needs. *Water Res* 2015;75:63–82.
- Frehland S, Kaegi R, Hufenus R, Mitran DM. Long-term assessment of nanoplastic particle and microplastic fiber flux through a pilot wastewater treatment plant using metal-doped plastics. *Water Res* 2020;182:115860.
- Gamarro G, Ryder, oll Ee, Olsen. Microplastics in fish and shellfish – a threat to seafood safety? *J Aquat Food Prod Technol* 2020;29(4):417–25.
- Gardon T, Morvan L, Huvet A, Quillien V, Soyez C, Le Moullac G, Le Luyer J. Microplastics induce dose-specific transcriptomic disruptions in energy metabolism and immunity of the pearl oyster *Pinctada margaritifera*. *Environ Pollut* 2020;266(Pt3):115180. <https://doi.org/10.1016/j.envpol.2020.115180>.
- Gavigan J, Kefela T, Macadam-Somer I, Suh S, Geyer R. Synthetic microfiber emissions to land rival those to waterbodies and are growing. *PLoS One* 2020;15(9): e0237839.
- Gallo F, Fossi C, Weber R, Santillo D, Sousa J, Ingram I, Nadal A, Romano D. Marine litter plastics and microplastics and their toxic chemicals components: the need for urgent preventive measures. *Environ Sci Eur* 2018;30(1):13.
- Grigorakis S, Mason SA, Drouillard KG. Determination of the gut retention of plastic microbeads and microfibers in goldfish (*Carassius auratus*). *Chemosphere* 2017;169:233–8.
- Hamed M, Soliman HAM, Osman AGM, Sayed AEH. Antioxidants and molecular damage in Nile Tilapia (*Oreochromis niloticus*) after exposure to microplastics. *Environ Sci Pollut Res Int* 2020;27(13):14581–8. <https://doi.org/10.1007/s11356-020-07898-y>.
- Hofmann AF. The continuing importance of bile acids in liver and intestinal disease. *Arch Intern Med* 1999;159:2647–58. <https://doi.org/10.1001/archinte.159.22.2647>.
- Hoffman MJ, Hittinger E. Inventory and transport of plastic debris in the Laurentian Great Lakes. *Mar Pollut Bull* 2017;115(1–2):273–81.
- Houten SM, Watanabe M, Auwerx J. Endocrine functions of bile acids. *EMBO J* 2006;25:1419–25.
- Huang JN, Wen B, Zhu JG, Zhang YS, Gao JZ, Chen ZZ. Exposure to microplastics impairs digestive performance, stimulates immune response and induces microbiota dysbiosis in the gut of juvenile guppy (*Poecilia reticulata*). *Sci Total Environ* 2020;733:138929.
- Hunt CF, Voulvoulis N. Chemical pollution of the aquatic environment and health. *Environmental Pollutant Exposures and Public Health*; 2020. p. 39–69.

- Jabeen K, Li B, Chen Q, Su L, Wu C, Hollert H, et al. Effects of virgin microplastics on goldfish (*Carassius auratus*). *Chemosphere* 2018;21:323–32. <https://doi.org/10.1016/j.chemosphere.2018.09.031>.
- Jambeck JR, Geyer R, Wilcox C, Siegler TR, Perryman M, Andrady A, Narayan R, Law KL. Plastic waste inputs from land into the ocean. *Science* 2015;347:768–71.
- Jiang M, Zhao HH, Zai SW, Shepherd B, Wen H, Deng DF. A defatted microalgae meal (*Haematococcus pluvialis*) as a partial protein source to replace fishmeal for feeding juvenile yellow perch *Perca flavescens*. *J Appl Phycol* 2019;31:1197–205.
- Jiang M, Zhao HH, Zai SW, Newton RJ, Shepherd B, Tian J, Lofald AG, Teh S, Binkowski FP, Deng DF. Nutritional quality of different starches in feed fed to juvenile yellow perch, *Perca flavescens*. *Aquacult Nutr* 2020;26(3):671–82.
- Jiang P, Yuan GH, Jiang BR, Zhang JY, Wang YQ, Lv HJ, Zhang Z, Wu JL, Wu Q, Li L. Effects of microplastics (MP) and tributyltin (TBT) alone and in combination on bile acids and gut microbiota crosstalk in mice. *Ecotoxicol Environ Saf* 2021;220:112345.
- Jin Y, Xia J, Pan Z, Yang J, Wang W, Fu Z. Polystyrene microplastics induce microbiota dysbiosis and inflammation in the gut of adult zebrafish. *Environ Pollut* 2018;235:322–9.
- Jovanović B, Gökdağ K, Güven O, Emre Y, Whitley EM, Kideys AE. Virgin microplastics are not causing imminent harm to fish after dietary exposure. *Mar Pollut Bull* 2018;130:123–31.
- Karami A, Golieskardi A, Choo CK, Romano N, Ho YB, Salamatinia B. A high-performance protocol for extraction of microplastics in fish. *Sci Total Environ* 2017;578:485–94.
- Kim J, Poirier DG, Helm PA, Bayoumi M, Rochman CM. No evidence of spherical microplastics (10–300 µm) translocation in adult rainbow trout (*Oncorhynchus mykiss*) after a two-wk dietary exposure. *PLoS One* 2020;15:e0239128.
- Kwon JH, Kim JW, Pham TD, Tarafdar A, Hong S, Chun SH, Lee SH, Kang DY, Kim JY, Kim SB, Jung J. Microplastics in food: a review on analytical methods and challenges. *Int J Environ Res Publ Health* 2020;17(18):6710.
- Lefebvre P, Cariou B, Lien F, Kuipers F, Staels B. Role of bile acids and bile acid receptors in metabolic regulation. *Physiol Rev* 2009;89(1):147–91.
- Lu Y, Yan Z, Deng Y, Jiang W, Zhao Y, Geng J, Ding L, Ren H. Uptake and accumulation of polystyrene microplastics in zebrafish (*Danio rerio*) and toxic effects in liver. *Environ Sci Technol* 2016;50(7):4054–60.
- Lusher A, Hollman P, Mendoza-Hill J. Microplastics in fisheries and aquaculture: status of knowledge on their occurrence and implications for aquatic organisms and food safety. *FAO*; 2017.
- Lyu W, Chen Q, Cheng L, Zhou W. Microplastics in aquaculture systems and their transfer in the food chain. *Microplast. Terrest. Environ.: Emerg Contam. Major Chall.* 2020;357e382.
- Marsden JE, Robillard SR. Decline of yellow perch in southwestern lake Michigan, 1987–1997. *N Am J Fish Manag* 2004;24(3):952–66.
- Martin M. Cutadapt removes adapter sequences from high-throughput sequencing reads. *Embnet Journal* 2011;17(1):10–2.
- Mercogliano R, Avio CG, Regoli F, Anastasio A, Colavita G, Santonicola S. Occurrence of microplastics in commercial seafood under the perspective of the human food chain. A review. *J Agric Food Chem* 2020;68(19):5296–301. <https://doi.org/10.1021/acs.jafc.0c01209>.
- Munro K, Helm PA, Rochman C, George T, Jackson DA. Microplastic contamination in Great Lakes fish. *Conserv Biol* 2021:1–11. <https://doi.org/10.1111/cobi.13794>.
- Negróni A, Cucchiara S, Stronati L. Apoptosis, necrosis, and necroptosis in the gut and intestinal homeostasis. *Mediat Inflamm* 2015;2015:250762. <https://doi.org/10.1155/2015/250762>. 10 pages.
- Nicholson JK, Foxall PJ, Spraul M, Farrant RD, Lindon JC. 750 MHz 1H and 1H-13C NMR spectroscopy of human blood plasma. *Anal Chem* 1995;67(5):793–811.
- Pedà C, Caccamo L, Fossi MC, Gai F, Andaloro F, Genovese L, et al. Intestinal alterations in European sea bass *Dicentrarchus labrax* (Linnaeus, 1758) exposed to microplastics: preliminary results. *Environ Pollut* 2016;212:251–6. <https://doi.org/10.1016/j.envpol.2016.01.083>.
- Piehl S, Leibner A, Löder MGJ, Dris R, Bogner C, Laforsch C. Identification and quantification of macro- and microplastics on an agricultural farmland. *Sci Rep* 2018;8:17950.
- Quast C, Pruesse E, Yilmaz P, Gerken J, Schweer T, Yarza P, Peplies J, Glöckner FO. The SILVA ribosomal RNA gene database project: improved data processing and web-based tools. *Nucleic Acids Res* 2013;41:D590–6.
- Rašković A, Stilić N, Kolarović J, Vasović V, Vukmirović S, Mikov M. The protective effects of silymarin against doxorubicin-induced cardiotoxicity and hepatotoxicity in rats. *Molecules* 2011;16(10):8601–13.
- Roch S, Brinker A. Rapid and efficient method for the detection of microplastic in the gastrointestinal tract of fishes. *Environ Sci Technol* 2017;51(8):4522–30.
- Rochman CM, Hentschel BT, Teh SJ. Long-term sorption of metals is similar among plastic types: implications for plastic debris in aquatic environments. *PLoS One* 2014;9(1):e85433.
- Rochman CM, Tahir A, Williams SL, Baxa DV, Lam R, Miller JT, Teh FC, Werorilangi S, Teh SJ. Anthropogenic debris in seafood: plastic debris and fibers from textiles in fish and bivalves sold for human consumption. *Sci Rep* 2015;5:14340.
- Sequeira IF, Prata JC, Costa JP, Duarte A, Rocha-Santos T. Worldwide contamination of fish with microplastics: a brief global overview. *Mar Pollut Bull* 2020;160:111681.
- Shapiro H, Kolodziejczyk AA, Halstuch D, Elinav E. Bile acids in glucose metabolism in health and disease. *J Exp Med* 2018;215(2):383–96.
- Smith M, Love DC, Rochman CM, Neff RA. Microplastics in seafood and the implications for human health. *Curr Env Health Rep* 2018;5:375–86.
- Sol D, Laca A, Laca A, Díaz M. Microplastics in wastewater and drinking water treatment plants: occurrence and removal of microfibrils. *Appl Sci* 2021;11:10109. <https://doi.org/10.3390/app112110109>.
- Sumner LW, Amberg A, Barrett D, Beale MH, Beger R, Daykin CA, Fan TWM, Fiehn O, Goodacre R, Griffin JL, Hankemeier T, Hardy N, Harnly J, Higashi R, Kopka J, Lane AN, Lindon JC, Marriott P, Nicholls AW, Reilly MD, Thaden JJ, Viant MR. Proposed minimum reporting standards for chemical analysis. *Metabolomics* 2007;3:211–21.
- Sussarellu R, Suquet M, Thomas Y, Lambert C, Fabioux C, Pernet MEJ, Goïc NL, Quillien V, Mingant C, Epelboin Y, Corporeau C, Guyomarch J, Robbens J, Paul-Pont I, Soudant P, Huvet A. Oyster reproduction is affected by exposure to polystyrene microplastics. *Proc Natl Acad Sci USA* 2016;113(9):2430–5.
- Tarnecki AM, Burgos FA, Ray CL, Arias CR. Fish intestinal microbiome: diversity and symbiosis unravelled by metagenomics. *J Appl Microbiol* 2017;123(1):2–17.
- Thiele CJ, Hudson MD, Russell AE, Saluveer M, Sidaoui-Haddad G. Microplastics in fish and fishmeal: an emerging environmental challenge? *Sci Rep* 2021;11:2045.
- Ulrich EL, Akutsu H, Doreleijers JF, Harano Y, Ioannidis YE, Lin JD, Livny M, Mading S, Mazuik D, Miller Z, Nakatani E, Schulte CF, Tolmie DE, Wenger RK, Yao HY, Markley JL. *BioMagResBank. Nucleic Acids Res* 2008;36:D402–8.
- Wagner M, Scherer C, Alvarez-Muñoz D, Brennholt N, Bourrain X, Buchinger S, Fries E, Grosbois C, Klasmeier J, Marti T, Rodriguez-Mozaz S, Urbatzka R, Vethaak AD, Winther-Nielsen M, Reifferscheid G. Microplastics in freshwater ecosystems: what we know and what we need to know. *Environ Sci Eur* 2014;26:12.
- Walkinshaw C, Lindeque PK, ThoMpon R, Tolhurst T, Cole M. Microplastics and seafood: lower trophic organisms at highest risk of contamination. *Ecotoxicol Environ Saf* 2020;190:110066.
- Wen B, Zhang N, Jin SR, Chen ZZ, Gao JZ, Liu Y, Liu HP, Xu Z. Microplastics have a more profound impact than elevated temperatures on the predatory performance, digestion and energy metabolism of an Amazonian cichlid. *Aquat Toxicol* 2018;195:67–76.
- Wilberg MJ, Bence JR, Eggold BT, Makauskas D, Clapp DF. Yellow perch dynamics in southwestern lake Michigan during 1986–2002. *N Am J Fish Manag* 2005;25(3):1130–52.
- Wishart DS, Jewison T, Guo AC, Wilson M, Knox C, Liu YF, Djoumbou Y, Mandal R, Aziat F, Dong E, Bouatra S, Sinelnikov I, Arndt D, Xia JG, Liu P, Yallou F, Bjorn Dahl T, Perez-Pineiro R, Eisner R, Allen F, Neveu V, Greiner R, Scalbert A. *Hmdb 3.0—the human metabolome database in 2013. Nucleic Acids Res* 2013;41:D801–7.
- Yu P, Liu Z, Wu D, Chen M, Lv W, Zhao Y. Accumulation of polystyrene microplastics in juvenile *Eriocheir sinensis* and oxidative stress effects in the liver. *Aquat Toxicol* 2018;200:28–36.
- Zeytin S, Wagner G, Mackay-Roberts N, Gerdt G, Schuirmann E, Klockmann S, Slater M. Quantifying microplastic translocation from feed to the fillet in European sea bass *Dicentrarchus labrax*. *Mar Pollut Bull* 2020;156:111210.
- Zha Y, Eiler A, Johansson F, Svanbäck R. Effects of food ration and predation stress on perch gut microbial communities. *Microbiome* 2018;6:28. <https://doi.org/10.1186/s40168-018-0400-0>.
- Zhang Y, Lee FY, Barrera G, Lee H, Vales C, Gonzalez FJ, Willson TM, Edwards PA. Activation of the nuclear receptor FXR improves hyperglycemia and hyperlipidemia in diabetic mice. *Proc Natl Acad Sci USA* 2006;103(4):1006–11.
- Zhang Y, Liang XF, He S, Chen X, Wang J, Li J, Zhu QS, Zhang Z, Li L, Alam MS. Effects of high carbohydrate diet-modulated microbiota on gut Health in Chinese perch. *Front Microbiol* 2020;11:2255.
- Zhu M, Chernick M, Rittschof D, Hinton DE. Chronic dietary exposure to polystyrene microplastics in maturing Japanese medaka (*Oryzias latipes*). *Aquat Toxicol* 2020;220:105396. <https://doi.org/10.1016/j.aquatox.2019.105396>.
- Zhu ZL, Wang SC, Zhao FF, Wang SG, Liu FF, Liu GZ. Joint toxicity of microplastics with triclosan to marine microalgae *Skeletonema costatum*. *Environ Pollut* 2019;246:509–17.